Enhancing pharmaceutical formulations to improve efficacy and delivery of drug molecules

by

Alisha K. Weight

B.A. Chemistry
Wellesley College, 2005

Submitted to the Department of Chemistry in Partial Fulfillment of the Requirements for the Degree of

Doctor of Philosophy in Biological Chemistry

at the

MASSACHUSETTS INSTITUTE OF TECHNOLOGY

ARCHIVES

June 2013

Signature of Author: _____
Department of Chemistry
March 5, 2013

Certified by: _____
Alexander M. Klibanov
Firmenich Professor of Chemistry and Bioengineering
Thesis Supervisor

Accepted by: _____
Robert W. Field
Haslam and Dewey Professor of Chemistry
Chairman, Departmental Committee on Graduate Students

This Doctoral Thesis has been examined by a committee of the Department of Chemistry as follows:

Barbara Imperiali
Class of 1922 Professor of Biology and Professor of Chemistry
Thesis Chair

Alexander M. Klibanov
Firmenich Professor of Chemistry and Bioengineering
Thesis Supervisor

Jianzhu Chen
Ivan R. Cottrell Professor of Immunology

Enhancing pharmaceutical formulations to improve efficacy and delivery of drug molecules

by

Alisha K. Weight

Submitted to the Department of Chemistry on March 5, 2013 in Partial Fulfillment of the Requirements for the Degree of Doctor of Philosophy in Biological Chemistry

Abstract

Major impediments to the full utility of current and potential drugs include issues of resistance and delivery. To address these challenges, in this thesis two directions of research were pursued: (1) the use of multivalent polymeric inhibitors to overcome drug resistance in human and avian influenza and (2) low-viscosity, high-concentration protein suspensions for therapeutic antibody, in particular monoclonal antibody (MAb), delivery.

(1) Influenza resistance to small molecule neuraminidase (NA) inhibitors is spreading. Little emphasis, however, has been placed on alternative formulations of inhibitors. We investigated the design of multivalent antivirals, wherein small molecule ligands of viral proteins are conjugated via a linker to a linear polymeric backbone.

Unexpectedly, we found that a poly-*L*-glutamine bearing pendant zanamivir (ZA) groups is at least as potent as those containing both ZA and sialic acid (SA). By examining the structure-activity relationship of such monofunctional conjugates, we show that the most potent one has 10% ZA attached to a neutral, high molecular weight backbone through a short alkyl linker. Importantly, we also demonstrate that such a polymer conjugate entirely compensates for weakened binding in and has 2,000-fold enhanced anti-viral potency against, ZA-resistant strains.

We further evaluated this optimized inhibitor *in vivo* and observed that it is an effective therapeutic of established infection in ferrets and reduces viral titers up to 190-fold when used as a combined prophylactic/therapeutic in mice. Additionally, we see no evidence that the conjugate stimulates an immune response in mice upon repeat administration.

(2) Typically, high doses of MAb therapeutics are required for clinical effect. Ideally, these MAbs would be delivered by subcutaneous injection of a small liquid volume. Such highly concentrated MAb solutions, however, are far more viscous than the 50 centipose (cP) permitted by the FDA. We evaluated approaches to reduce formulation viscosity by forming protein suspensions. Aqueous suspensions induced by poly(ethylene glycol), precipitating salts, or ethanol actually increased viscosity. However, non-aqueous suspensions of amorphous antibody powders in organic solvents that have ≤ 1 hydrogen atom available for hydrogen-bonding, exhibited up to a 38-fold decrease in viscosity.

Thesis Supervisor: Alexander M. Klibanov
Title: Firmenich Professor of Chemistry and Bioengineering

Acknowledgements

My deepest gratitude to Professor Alexander Klibanov for the gift of time. Your guidance has made me a more independent and deliberate researcher, and a more assertive, effective advocate. You have shaped and broadened my perspectives in science and for life.

I would also like to acknowledge my committee members, Professors Jianzhu Chen and Barbara Imperiali. Jianzhu, thank you for your patient guidance on my project and making me feel like a member of your lab. Barbara, thank you for your thoughtful support, both scientifically and personally, and allowing me to use your lab space and equipment.

I could not have completed this work without all the current and former members of the Klibanov and Chen groups. In particular, I thank Jen Fortune, Eugene Antipov, Bryan Hsu, Alyssa Larson, Adam Drake, Steve Chen, Mobolaji Olurinde, and Jaimie Lee for many years of helpful and stimulating discussions, research-related and not. To my friends outside these labs, thank you for your constant encouragement and support.

Last, but not least, I am eternally grateful to my parents. Your endless love and pragmatic encouragement have made my successes sweeter and failures less bitter.

Table of Contents

Abstract	3
Acknowledgements	4
Table of Contents	5
List of Figures	6
List of Tables	7
Abbreviations	8
I. Influenza Virus and Current Treatments	
A. Introduction	10
B. References	15
II. Polymer-attached zanamivir inhibits drug-resistant strains of influenza A virus	
A. Introduction	21
B. Results and Discussion	23
C. Materials and Methods	39
D. References	45
III. Polymer-attached zanamivir is both an effective prophylactic and therapeutic *in vivo*	
A. Introduction	50
B. Results and Discussion	51
C. Materials and Methods	56
D. References	61
IV. Reducing the viscosity of highly concentrated antibody formulations	
A. Introduction	65
B. Results and Discussion	66
C. Materials and Methods	80
D. References	85
Appendix	87

List of Figures

Figure 1-1	Infection cycle of influenza virus and point of action of current therapies	11
Figure 1-2	Mechanism of action of viral NA	12
Figure 1-3	Chemical structures of approved and experimental small-molecule NA inhibitors	14
Figure 2-1	Illustration of proposed multivalent inhibition	22
Figure 2-2	Scheme of synthetic route to ZA-derivatized poly-*L*-glutamines	24
Figure 2-3	Antiviral activity enhancements of polymeric inhibitor **12b** against drug resistant influenza strains	30
Figure 2-4	Antiviral activities of monofunctional ZA-containing polymeric inhibitors with varying percent derivatization	31
Figure 2-5	Synthetic scheme and chemical structures of polymer-ZA conjugates varying in linker group and backbone properties	32
Figure 2-6	Antiviral activities of ZA analogs and their polymer-attached derivatives	33
Figure 2-7	Inhibitory potencies of polymer-ZA conjugates varying in backbone charge and molecular weight	34
Figure 2-8	Experimental design to assay for inhibitory potency in the plaque reduction assay during early or all stages of infection	37
Figure 2-9	Synthetic scheme of silver-mediated SA linker attachment	40
Figure 3-1	Chemical structures of compounds used *in vivo*	51
Figure 3-2	Experimental design for and efficacy of polymeric inhibitor **12b** in mice	53
Figure 3-3	Experimental design for and efficacy of polymeric inhibitor **12b** in ferrets	54
Figure 4-1	Dependence of viscosities of γ-globulin solutions on protein concentration	67
Figure 4-2	Dependence of viscosities of γ-globulin suspensions on % ethanol	72
Figure 4-3	Temperature dependence of viscosities of γ-globulin solutions and neat ethanol suspensions.	74
Figure 4-4	Chemical structures of organic solvents used to suspend γ-gloublin	77
Figure 4-5	Sample viscosity plots: Newtonian and non-Newtonian behavior	81

List of Tables

Table 2-1	Antiviral activities of ZA-containing inhibitors	26
Table 2-2	Antiviral activities of bifunctional polymeric inhibitors	28
Table 2-3	Inhibition of drug-resistant NA enzymes by ZA-containing inhibitors	36
Table 2-4	Antiviral activities of **12b** and ZA present during different stages of infection	38
Table 3-1	Immunogenicity of intranasal delivery of polymeric inhibitor **12b** in mice	55
Table 4-1	Viscosities and particle sizes of γ-globulin solution before and after aqueous suspension	68
Table 4-2	Viscosities of aqueous γ-globulin formulations with added surfactants	69
Table 4-3	Viscosities of aqueous γ-globulin formulations with added salts	70
Table 4-4	Viscosities of aqueous γ-globulin formulations with added arginine salts	70
Table 4-5	Viscosities and particle sizes of aqueous γ-globulin formulations with arginine acetate	71
Table 4-6	Viscosities and particle sizes of aqueous ethanol nanosuspensions of γ-globulin	71
Table 4-7	Viscosities and particle sizes of neat ethanol suspensions of commercial and ethanol-precipitated γ-globulin	73
Table 4-8	Viscosities of γ-globulin suspensions in a variety of neat organic solvents	76
Table 4-9	Viscosities of monoclonal antibody suspensions in neat organic solvents	78

Abbreviations

Standard 1-letter codes are used for amino acids.

HA	influenza hemagglutinin protein
IC_{50}	50% maximal inhibitory concentration
M2	influenza matrix protein 2
NA	influenza neuraminidase enzyme
Nanchang	influenza strain A/Nanchang/933/95
PIBMA	poly(isobutylene-*alt*-maleic anhydride)
pfu	plaque forming units, a unit of viral titer
PR8	influenza strain A/PR/8/34
SA	sialic acid
SAR	structure activity relationship
TKY	avian influenza A/turkey/MN/833/80
TKY E119D	avian influenza A/turkey/MN/833/80 with ZA-resistant mutation E119D
TKY E119G	avian influenza A/turkey/MN/833/80 with ZA-resistant mutation E119G
Victoria	influenza A/Victoria/3/75
WSN	influenza A/WSN/33
Wuhan	influenza A/Wuhan/359/95
Wuhan E119V	influenza A/Wuhan/359/95 with oseltamivir-resistant mutation E119V
ZA	zanamivir (Relenza™)

cP	centipoise (a unit of viscosity)
MAb	monoclonal antibody
SMAb	murine monoclonal antibody from the company Sanofi-Aventis
NMAb	humanized monoclonal antibody from the company Novartis

Chapter 1: Influenza virus and current treatments

A. Introduction

Epidemiology of Influenza

Yearly outbreaks of influenza affect approximately 20% of the world's population[1-4b] and result in hundreds of thousands of deaths each year[2,3]. Population growth and the convenience of international travel have contributed to the increased incidence of influenza pandemics[5]. Many of these pandemic viruses are human-infectious reassortment strains that typically develop upon co-infection of a host species with both an animal and a human strain[6,7]. Such inter-species reassortment is also known as antigenic shift, and results in the expression of novel surface antigens to which the human population is frequently serologically naive[6-8]. These new variants heighten the risk of severe illness and pandemic[6,8]. Additional variation arises from antigenic drift, the result of drug and immune pressure and the rapid random mutation rate of RNA viruses such as influenza[9]. The accelerated emergence and recognition of drug-resistant strains and, since 1997 the increased frequency of animal-to-human transmission of novel and/or highly pathogenic strains[7,8], underscore the necessity for anti-influenza therapies to combat both avian viruses and drug resistance.

Biochemistry of Influenza Infection

Influenza virus belongs to the *Orthomyxoviridae* family of enveloped RNA viruses. Three surface proteins integral to viral infection and replication have been targeted by influenza treatments: major antigen hemagglutinin (HA), matrix protein 2 (M2), and minor antigen neuraminidase (NA).

Each subunit of the non-covalently linked HA homotrimer has a conserved receptor-binding pocket that recognizes cell-surface sialic acids (SA)[9]. Non-conserved regions of HA determine increased binding affinity to either α-2,3- or α-2,6-linked SA,

found predominantly on avian or human cells, respectively[6,10,11]. Recently, however, α-2,3-linked terminal SA was found to be more abundant in the human respiratory tract than previously thought, perhaps explaining why avian-mammal re-assortment strains can cause human epidemics[10,11].

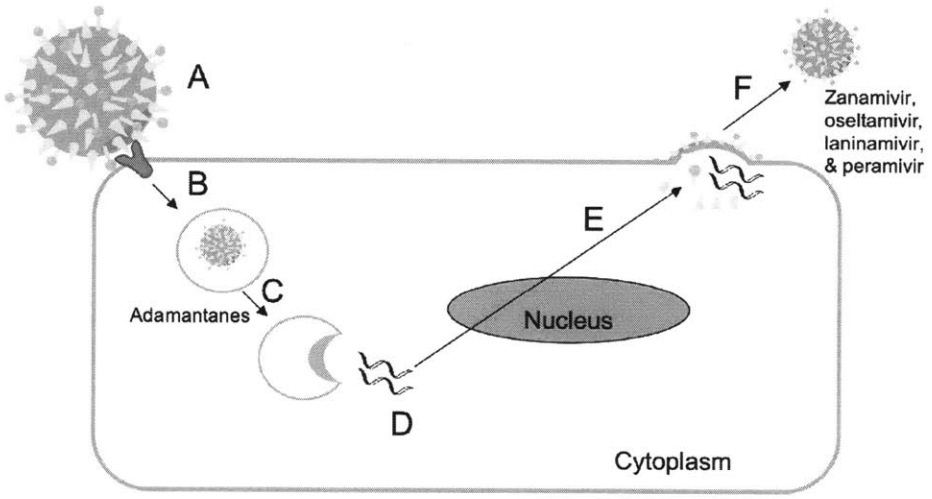

Figure 1-1. Infection cycle of influenza virus and points of action of current therapies. Virion (**A**) displays HA (cone shaped spikes) and NA (stalks with bulbous heads) proteins. Low-affinity HA interactions with cell surface SA lead to endocytosis (**B**). Upon acidification of the virion via the M2 ion channel, HA irreversibly fuses with the endosomal membrane (**C**), releasing viral nucleocapsid (**D**) for unpackaging. After transcription and protein synthesis, all components of the new virion are assembled at the cell membrane (**E**). The virion buds from the cell membrane and NA cleaves SA from the cell surface (**F**), releasing the viral particle to infect more cells.

Low affinity (K_d = 1 mM) high avidity interactions of cellular SA and viral HA stimulate receptor-mediated endocytosis of influenza virions[9,12] (Fig 1-1B). Acidification of the endosome by cellular H^+-ATPases and the inside of the virion by the viral proton-selective M2 ion channel, leads to irreversible structural changes in HA followed by virus-endosome fusion[9,13] (Fig 1-1C). Subsequent release of viral nucleocapsids into the cellular cytosol introduces viral RNA into the cell[9,14] (Fig 1-1D).

At approximately four hours, after replication of viral RNA and viral particle assembly at the apical surface of the infected cell, new virions bud from the cellular

membrane[6,9] (Fig 1-1E). Viral enzyme NA cleaves the terminal α-ketosidic linkage between SA and D-galactose or D-galactosamine on cell-surface glycoproteins and glycolipids (Fig 1-1F). The influenza NA homotetramer preferentially catalyzes the hydrolysis of α-2,3 and α-2,6 glycosidic bonds (Fig 1-2) through which virions are non-covalently bound to a cell surface[6,10,11].

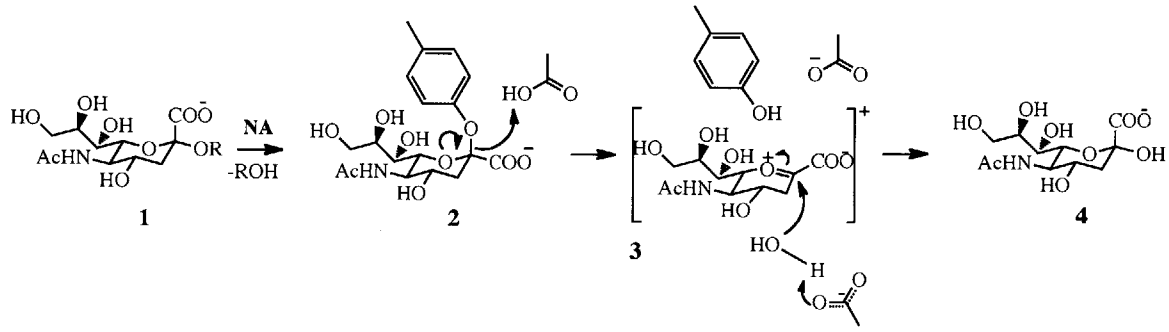

Figure 1-2. Viral NA catalyzes ketosidic bond cleavage of terminal SA (**1**) through a covalent intermediate (**2**) and oxocarbonium transition state (**3**) to generate free α-sialic acid with retention of stereochemistry (**4**).

This enzymatic activity, in abolishing multivalent HA-SA interactions, speeds release of new virions to infect adjacent cells, thus promoting multicycle infection[9,10,15,16]. NA activity also prevents virion aggregation during budding and degrades host mucins to enable viral access to epithelial cell surfaces[9,17,18]. Whether these three actions are critical to infection or whether they merely promote it is controversial[15,17-19]. All influenza NA share eighteen highly conserved residues in the active site: eight functional and ten structural[20,21,22].

Antigenic classification of HA and NA proteins – i.e., H1N1 – is widely used to discuss influenza viruses, and provides information on host species and potential pathogenicity. Such categorization is based not on sequence homology, but on binding to subtype-specific anti-HA and anti-NA antibodies in a double immunodiffusion assay[23].

H1N1 and H3N2 strains are the most common human infectious strains that cause the bulk of morbidity during yearly outbreaks, and are always targeted in annual vaccinations[6,24].

Treatments for influenza

Currently, only two treatment modalities are available for influenza infection: immunization and small molecule inhibitors. Prophylactic seasonal immunization with a vaccine against three subtypes of major surface antigen HA is up to 70% effective in the non-elderly and immune-competent populations[24] but relies on accurate prediction of future circulating strains. Antigenic shift or inaccurate strain selection make the vaccine even less efficacious. Though they are costly, have many side effects, and have a small therapeutic window, broader-spectrum small molecule inhibitors targeting the M2 and NA proteins of all influenza strains have been developed to prevent and control disease when the vaccine is least effective[24-26].

Inhibition of the M2 ion channel by the adamantane class of drugs prevents release of RNA from viral nucleocapsid complexes, thus halting replication[9] (Fig 1-1C). Recently, however, the FDA has recommended against use of the these inhibitors as most circulating influenza A viruses are now resistant to them[27,28], and resistant mutations have even been identified in highly pathogenic H5N1 strains isolated from treated patients[29].

Fewer resistant strains of influenza are identified after treatment with the NA inhibitors zanamivir (**5**, ZA; Relenza™) and oseltamivir (**6**, Tamiflu™), two SA transition-state analogs (Fig 1-3). Resistance to oseltamivir is now commonly identified in both treated patients and circulating strains[4b,27,30-32] though the prevalence of such resistance varies from season to season[28]. Mutations conferring resistance to ZA appear

less frequently. Though such mutations reduce enzymatic activity, their effects on viral fitness (i.e. ability to infect, replicate, and re-infect) are unresolved[33,34].

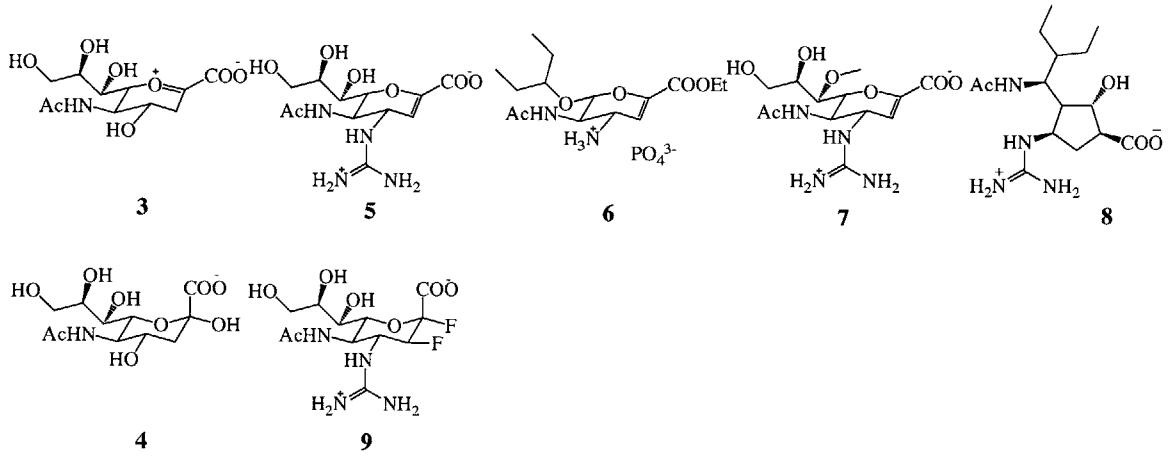

Figure 1-3. Chemical structures of NA inhibitors. Approved inhibitors include analogs of the NA-induced SA transition state (**3**) including ZA (**5**), oseltamivir (**6**), and prodrug laninamivir (**7**). Peramivir (**8**) has characteristics of both **5** and **6**. Novel analogs of the α-anomer of SA (**4**) including 2α-3_{eq}-4-guanidino-difluorosialic acid (**9**) have been recently identified as highly effective covalent NA inhibitors.

Though there is a high degree of conservation in and around the NA active site, mutations conferring resistance to oseltamivir and ZA typically arise at structural residues in a subtype specific manner, commonly at H274 in N1 enzymes (oseltamivir-resistant) and at R292 or E119 in N2 enzymes (oseltamivir- and ZA-resistant, or just ZA-resistant, respectively)[21,31,35]. The highly potent NA inhibitors laninamivir (**7**) and peramivir (**8**) (Fig 1-3) are still undergoing FDA approval but were widely used during the 2009 pandemic under temporary emergency authorization[36]. However, Cross-resistance to NA-inhibitor-resistant strains has been observed with these newer drugs as they too inhibit NA[36,37]. The search for small molecule inhibitors designed to circumvent or prevent drug resistant mutations is ongoing against current[31,38-42] and novel[28,43-45] targets. For example, a recent report identified a new class of mechanism-based SA

analogs such as **9** that show no cross-resistance, effectively inhibiting drug-resistant NA mutants up to 40-fold better than ZA by trapping covalent intermediate **2** (Figure 1-2)[42].

Work in our lab and others has shown that macromolecules – as opposed to small molecules – are typically more potent inhibitors of influenza infection. These inhibitors comprise recombinant proteins[7,46], and derivatized polypeptides[47,48] or synthetic polymers[49-52]. In the coming chapters we build on previous work with derivatized synthetic polymers and explore the benefits of such an alternative approach, including facile structure optimization, broad-spectrum inhibition of drug-susceptible and drug-resistant strains, and *in vivo* prophylactic and therapeutic efficacy.

B. References

1. Luscher-Mattlie M, Influenza chemotherapy: A review of the present state of art and of new drugs in development. *Arch Virol*, **2000**, 145, 2233–2248.
2. Dushoff J, Plotkin JB, Viboud C, Earn DJD, Simonsen L, Mortality due to Influenza in the United States – An Annualized Regression Approach Using Multiple-Cause Mortality Data. *Am J Epi*, **2005**, 163, (2), 181-187.
3. Graham-Rowe D, Racing against the flu. *Nature*, **2011**, 480, S2–S3.
4. (a) Moscona A, Oseltamivir resistance—disabling our influenza defenses. *New Engl J Med*, **2005**, 353, 2633–2636; (b) Moscona A, Global transmission of oseltamivir-resistant influenza. *New Engl J Med*, **2009**, 360, (1), 953-956.
5. Centers for Disease Control and Prevention. Epidemiology and Prevention of Vaccine-Preventable Diseases. Atkinson W., Hamborsky J., McIntyre L., Wolfe S., eds. 10th Ed. Washington DC: Public Health Foundation. **2007**
6. "Virology of Human Influenza." Influenza Report 2006. Paris: Flying Publisher. **2006**.
7. Triana-Baltzer GB, Gubareva LV, Nicholls JM, Pearce MB, Mishin VP, Belser JA, Chen L-M, Chan RWY, Chan MCW, Hedlund M, Larson JL, Moss RB, Katz JM, Tmpey TM, Fang G, Novel Pandemic Influenza A (H1N1) Viruses Are Potently Inhibited by DAS181, a Sialidase Fusion Protein. *PLoS ONE,* **2009**, 4, (11), e7788.
8. World Health Organization. H5N1 Avian Influenza: Timeline of major events. 2 April **2007**.
9. "*Orthomyxoviridae*: The Viruses and Their Replication." Fields Virology. Lamb RA and Krug RM eds. 4th Ed (Illustrated). Lippincott, Williams, and Wilkins, Philadelphia, PA. **2001**.
10. Nicholls JM, Bourne AJ, Chen H, Guan Y, Malik Peiris JS, Sialic acid receptor

detection in the human respiratory tract: evidence for widespread distribution of potential binding sites for human and avian influenza viruses. *Resp Res*, **2007**, 8, 73.

11. Gambaryan AS, Tuzikov AB, Pazynina GV, Webster RG, Matrosovich MN, Bovin NV, H5N1 chicken influenza viruses display a high binding affinity for Neu5Acalpha2-3Galbeta1-4(6-HSO3)GlcNAc-containing receptors. *Virology*, **2004**, 326, 310-316.
12. Glick GD, Toogood PL, Wiley DC, Skehel JJ, Knowles JR, Ligand recognition by influenza virus. The binding of bivalent sialosides. *J Biol Chem*, **1991**, 266, 23660-23669.
13. Skehel JJ and Wiley DC, Receptor binding and membrane fusion in virus entry: the influenza hemagglutinin. *Ann Rev Biochem*, **2000**, 69, 521-569.
14. Carr CM, Chaudhry C, Kim PS, Influenza hemagglutinin is spring-loaded by a metastable native conformation. *Proc Nat Acad Sci*, **1997**, 94, 14306-14313.
15. Palmer, Lines of defense. *Nature*, **2011**, 480, S9–S10.
16. Liu C, Eichelberger MC, Compans RW, Air GM, Influenza type A virus neuraminidase does not play a role in viral entry, replication, assembly, or budding. *J Virol*, **1995**, 69, 1099–1106.
17. McNicholl IR, McNicholl JJ, Neuraminidase inhibitors: zanamivir and oseltamivir. *Ann Pharmacother*, **2001**, 35, 57-70.
18. Matrosovich MN, Matrosovich TY, Gray T, Roberts NA, Klenk H-D, Neuraminidase is important for the initiation of influenza virus infection in human airway epithelium. *J Virol*, **2004**, 78, 12665–12667.
19. Greengard O, Poltoratskaia N, Leikina E, Zimmerberg J, Moscona A, The anti-influenza virus agent 4-GU-DANA (zanamivir) inhibits cell fusion mediated by human parainfluenza virus and influenza virus HA. *J Virol*, **2000**, 74, 11108–11114.
20. Varghese JN, Epa VC, Colman PM, Three-dimensional structure of the complex of 4-guanidino-Neu5Ac2en and influenza virus neuraminidase. *Protein Sci,* **1995**, 4, 1081-1087.
21. Yen H-L, Hoffmann E, Taylor G, Scholtissek C, Monto AS, Webster RG, Govorkova EA, Importance of Neuraminidase Active-Site Residues to the Neuraminidase Inhibitor Resistance of Influenza Viruses. *J Virol*, **2006**, 80, (17), 8787-8795.
22. von Itzstein M, The war against influenza: Discovery and development of sialidase inhibitors. *Nat Rev Drug Discov*, **2007**, 6, (12), 967–974.
23. Fouchier RAM, Munster V, Wallenstein A, Bestebroer TM, Herfst S, Smith D, Rimmelzwaan GF, Olsen B, Osterhaus ADME, Characterization of a Novel Influenza A virus Hemagglutinin Subtype (H16) Obtained from Black-Headed Gulls. *J Virol*, **2005** ,79, (5), 2814-2822.
24. Centers for Disease Control. Prevention and Control of Influenza: Recommendations of the Advisory Committee on Immunization Practices. *MMWR*, **2006**, 55, (RR10), 1-42.
25. De Clercq E, Antiviral agents active against influenza A viruses. *Nat Rev Drug Discov*, **2006**, 5, (12), 1015–1025.
26. Lipatov AS, Govorkova EA, Webby RJ, Ozaki H, Peiris M, Guan Y, Poon L,

Webster RG, Influenza: Emergence and control. *J Virol*, **2004**, 78, (17), 8951–8959.

27. World Health Organization. Weekly epidemiological record 4 November 2011. **2011**, 45, (86), 497-508.
28. Ortigoza MB, Dibben O, Maamary J, Martinez-Gil L, Leyva-Grado VH, Abreu P, Ayllon J, Palese P, Shaw ML, A novel small molecule inhibitor of influenza A viruses that targets polymerase function and indirectly induces interferon. *PLoS Pathog*, **2012**, 8, (4), e1002668.
29. de Jong MD, Tran TT, Khanh TH, Hien, VM, Smith GJD, Nguyen VC, Bach VC. Phan TQ, Do QH, Guan Y, Peiris JSM, Tran TH, Oseltamivir resistance during treatment of influenza A (H5N1) infection. *N Engl J Med,* **2005**, 353, 2667–2672.
30. Kiso M, Mitamura K, Sakai-Tagawa, Y, Shiraishi K, Kawakami C, Kimura K, Hayden FG, Sugaya N, Kawaoka Y, Resistant influenza A viruses in children treated with oseltamivir: descriptive study. *N Eng J Med*, **2004**, 364, 759-765.
31. Mishin VP, Hayden FG, Gubareva LV, Susceptibilities of antiviral-resistant influenza viruses to novel neuraminidase inhibitors. *Antimicrob Agents Chemother*, **2005**, 49, 4515–4520.
32. Thorlund K, Awad T, Boivin G, Thabane L, Systematic review of influenza resistance to the neuraminidase inhibitors. *BMC Infetct Dis*, **2011**, 11, 134.
33. Hurt AC, Holien JK, Parker M, Kelso A, Barr IG, Zanamivir-resistant influenza viruses with a novel neuraminidase mutation. *J Virol*, **2009**, 83, (20), 10366-10373.
34. Zurcher T, Yates J, Daly J, Sahasrabudhe A, Walters M, Dash L, Tisdale M, McKimm-Breschkin JL, Mutations conferring zanamivir resistance in human influenza virus N2 neuraminidases compromise virus fitness and are not stably maintained *in vitro*. *J Antimicrob Chemo*, **2006**, 58, 723-732.
35. Abed Y, Baz M, Boivin G, Impact of neuraminidase mutations conferring influenza resistance to neuraminidase inhibitors in the N1 and N2 genetic backgrounds. *Antiviral Therapy*, **2006**, 11, 971-976.
36. Administration USFaD. FDA authorized emergency use of intravenous antiviral peramivir for 2009 H1N1 influenza for certain patients, settings. **2009**, (U.S. Food and Drug Administration), FDA NOTE TO CORRESPONDENTS. http://www.fda.gov/downloads/Drugs/DrugSafety/PostmarketDrugSafetyInformationforPatientsandProviders/UCM187811.pdf
37. Gubareva LV, Webster RG, Hayden FG, Comparison of the activities of zanamivir, oseltamivir, and RWJ-270201 against clinical isolates of influenza virus and neuraminidase inhibitor-resistant variants. *Antimicrob Agents Chemother*, **2001**, 45, (12), 3403-3408.
38. Koyama K, Takahashi M, Oitate M, Nakai N, Takakusa H, Miura S, Okazaki O, CS-8958, a prodrug of the novel neuraminidase inhibitor R-125489, demonstrates a favorable long-retention profile in the mouse respiratory tract. *Antimicrob Agents Chemother*, **2009**, 53, 4845–4851.
39. An J, Lee DCW, Law AHY, Yang CLH, Poon LLM, Lau ASY, Jones SJM, A novel small-molecule inhibitor of the avian influenza H5N1 virus determined through computational screening against the neuraminidase. *J Med Chem*, **2009**,

52, 2667-2672.

40. Hashem AM, Flaman AS, Farnsworth A, Brown EG, Van Domselaar G, He R, Li X, Aurintricarboxylic Acid Is a Potent Inhibitor of Influenza A and B Virus Neuraminidases. *PLoS ONE*, **2009**, 4, (12), e8350.
41. Yamashita M, Tomozawa T, Kakuta M, Tokumitsu A, Nasu H, Kubo S, CS-8958, a prodrug of the new neuraminidase inhibitor R-125489, shows long-acting anti influenza virus activity. *Antimicrob Agents Chemother*, **2009**, 53, (1), 186-192.
42. Kim J-H, Resende R, Wennekes T, Chen H-M, Bance N, Buchini S, Watts AG, Pilling P, Streltsov VA, Petric M, Liggins R, Barrett S, McKimm-Breschkin JL, Niikura M, Withers SG, Mechanism-Based Covalent Neuraminidase Inhibitors with Broad Spectrum Influenza Antiviral Activity. *Science*. **2013**, Early online publication 21 February 2013.
43. Jablonski JJ, Basu D, Engel DA, Geysen HM, Design, synthesis, and evaluation of novel small molecule inhibitors of the influenza virus protein NS1. *Bioorg Med Chem,* **2012**, 20, 487-497.
44. Muratore G, Goracci L, Mercorelli B, Foeglein A, Digard P, Cruciani G, Palu G, Loregian A, Small molecule inhibitors of influenza A and B viruses that act by disrupting subunit interactions of the viral polymerase. *Proc Nat Acad Sci USA*, **2012**, 109, (16), 6247-6252.
45. Garcia-Sosa AT, Sild S, Maran U, Design of multibinding- site inhibitors, ligand efficiency, and consensus screening of avian influenza H5N1 wild-type neuraminidase and of the oseltamivir-resistant H274Y variant. *J Chem Inf Model*, **2008**, 48, 2074–2080.
46. Belser J, Lu X, Szretter KJ, Jin X, Aschenbrenner LM, Lee A, Hawley S, Kim do H, Malakhov MP, Yu M, Fang F, Katz JM, DAS181, A novel sialidase fusion protein, protects mice from lethal avian influenza H5N1 virus infection. *J Infect Dis*, **2007**, 196, (10), 1493-1499.
47. Masuda T, Yoshida S, AraiM, Kaneko S, Yamashita M, Honda T, Synthesis and anti-influenza evaluation of polyvalent sialidase inhibitors bearing 4-guanidino-Neu5Ac2en derivatives. *Chem Pharm Bull*, **2003**, 51, 1386–1398.
48. Roy R, Pon RA, Tropper RD, Andersson FO, Michael addition of poly-L-lysine to *N*-acryloylated sialosides. Syntheses of influenza A virus haemagglutinin inhibitor and group B meningococcal polysaccharides vaccines. *J Chem Soc Chem Commun*, **1993**, 3, 264-265.
49. Haldar J, Alvarez de Cienfuegos L, Tumpey TM, Gubareva LV, Chen J, Klibanov AM. Bifunctional polymeric inhibitors of human influenza A viruses. *Pharm Res*, **2010**, 27, 259–263.
50. Mammen M, Dahmann G, Whitesides GM, Effective inhibitors of hemagglutination by influenza virus synthesized from polymers having active ester groups. *J Med Chem*, **1995**, 38, 4179–4190.
51. Sigal GB, Mammen M, Dahmann G, Whitesides, Polyacrylamides bearing pendant α-sialoside groups strongly inhibit agglutination of erythrocytes by influenza virus: the strong inhibition reflects enhanced binding through cooperative polyvalent interactions. *J Am Chem Soc*, **1996**, 118,3789-3800.
52. Gambaryan AS, Boravleva EY, Matrosovich TY, Matrosovich MN, Klenk H-D, Moiseeva EV, Tuzikov AB, Chinarev AA, Pazynina GV, Bovin NV, Polymer-

bound 6' sialyl-*N*-acetyllactosamine protects mice infected by influenza virus. *Antiviral Res*, **2005**, 68, 116-123.

Chapter 2: Polymer-attached zanamivir inhibits drug-resistant strains of influenza A virus

Much of the work described in this chapter was/will be published in the following manuscripts:

Weight AK, Haldar J, Alvarez de Cienfuegos L, Gubaerva LV, Tumpey TM, Chen J, Klibanov AM, Attaching zanamivir to a polymer markedly enhances its activity against drug-resistant strains of influenza A virus. **2011**, *J Pharm Sci*, 100, (3), 831-835.

Weight AK, Belser JA, Tumpey TM, Chen J, Klibanov AM, Zanamivir conjugated to poly-*L*-glutamine is much more active against influenza viruses in mice and ferrets than the drug itself. **2013**, *J Pharm Sci*. Submitted.

A. INTRODUCTION

Drug resistance is a rapidly evolving threat to global human health. Though the prevalence of drug-resistant mutations varies seasonally, current treatments are often rendered entirely ineffective[1-3]. Therapeutics that inhibit all strains of influenza – both drug-susceptible and drug-resistant – are urgently needed, and small-molecule discovery has not yet successfully addressed the issue.

Macromolecular and multivalent inhibitors of influenza

Macromolecular inhibitors – either proteins or synthetic polymers – offer a promising alternative paradigm. In particular, they hold promise as broad-spectrum inhibitors that can address issues of drug resistance. For example, the fusion sialidase DAS181 (Fludase™) removes cell-surface sialic acid (SA) in the airways to prevent the viral attachment to cellular hemagglutinin (HA) receptors that initiates infection[4-6]. Though low-level resistance to DAS181 has been observed, it appears to be reversible upon removal of treatment[7].

Another way to prevent these numerous HA-SA interactions is to harness that same multivalency – the interaction of multiple copies of a ligand (i.e., SA) with multiple copies of a target protein (i.e., HA) – in a synthetic inhibitor[8] (Fig 2-1). By attaching analogs of SA[9-11] or sialyloligosaccharides[12] to polymer scaffolds, such conjugates can mimic a cell surface, "trapping" a virus via multivalent binding before infection occurs.

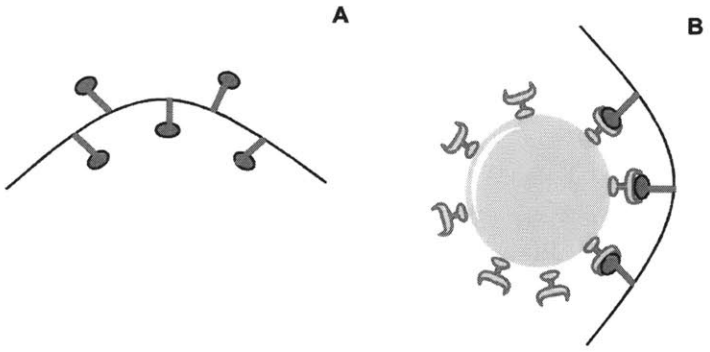

Figure 2-1. Schematic illustration of proposed multivalent inhibition. (**A**) A flexible polymer scaffold (curved black line) bearing pendant groups (gray ovals) attached through flexible linkers (gray sticks) (**B**) participates in a multivalent interaction with receptors on the surface of a viral particle.

Indeed, such multivalent inhibitors showed enhanced inhibition of virion binding to cell-surface SA in an erythrocyte sedimentation assay[9-11,13] and inhibition of viral infection in cell culture[14]. Both the polyacrylamide/polyacrylate[9-11] and polystyrene[15] backbones primarily used in those studies, however, are not amenable to drug development due to *in vivo* acrylamide toxicity[16,17], *in vitro* polyacrylamide toxicity at inhibitory concentrations[17,18], and poor water solubility[13]. Sialyloligosaccharides conjugated to biocompatible scaffolds such as dendrimeric polyethylenimine[19] and poly-*L*-lysine[20], or linear poly-*L*-glutamic acid[18,20,21] showed up to 20-fold enhanced inhibition of infection. Analogously, multivalent NA inhibitors composed of poly-*L*-glutamine[22,23] or oxidized dextran[24] bearing pendant zanamivir (ZA) groups demonstrated increased potency in cell culture compared to small molecule ZA itself.

Another potential benefit of polymeric inhibitors is the coupling of multivalency and combination therapy, which is known to reduce the emergence of drug-resistant pathogens[25]. Previously in our lab, a bifunctional inhibitor – a single polymer bearing multiple different ligands of viral proteins, i.e., SA and ZA – that has multiple modes of

action, was shown to synergistically enhance efficacy compared to a polymer with ZA alone[26]. Such inhibitors, however, were based on the biodegradable but potentially immunogenic hydrolyzed poly(isobutylene-*alt*-maleic anhydride) backbone (PIBMA)[27]. Although multivalent ZA-containing inhibitors possess enhanced potency against select wild-type human strains of influenza virus[22,23,26], their efficacy against a range of subtypes and drug sensitivities has not been explored.

Project preview

Expanding upon the aforementioned studies, in this chapter we 1) show that across numerous influenza subtypes and strains, monofunctional ZA-derivatized polymers are at least as efficacious as bifunctional inhibitors, 2) optimize the percent ZA, linker group, and polymer backbone of such a monofunctional inhibitor through *in vitro* structure activity relationship (SAR) studies, and 3) demonstrate that attaching ZA to a polymer backbone can overcome both oseltamivir and ZA resistance in not only human but also avian strains. Additionally, in Chapter 3, we present preliminary *in vivo* data assessing efficacy and immunogenicity of the optimized ZA-derivatized inhibitor identified herein.

B. RESULTS AND DISCUSSION

Bifunctionally derivatized polypeptides show neither additive nor synergistic inhibition

First, to explore the benefits of multivalent ZA-derivatized polymers, we selected poly-*L*-glutamate as the starting material for synthesis of our inhibitors. Poly-*L*-glutamate, which is commercially available in a range of molecular weights, has been used safely *in vivo*[28,29] and is readily modified synthetically.

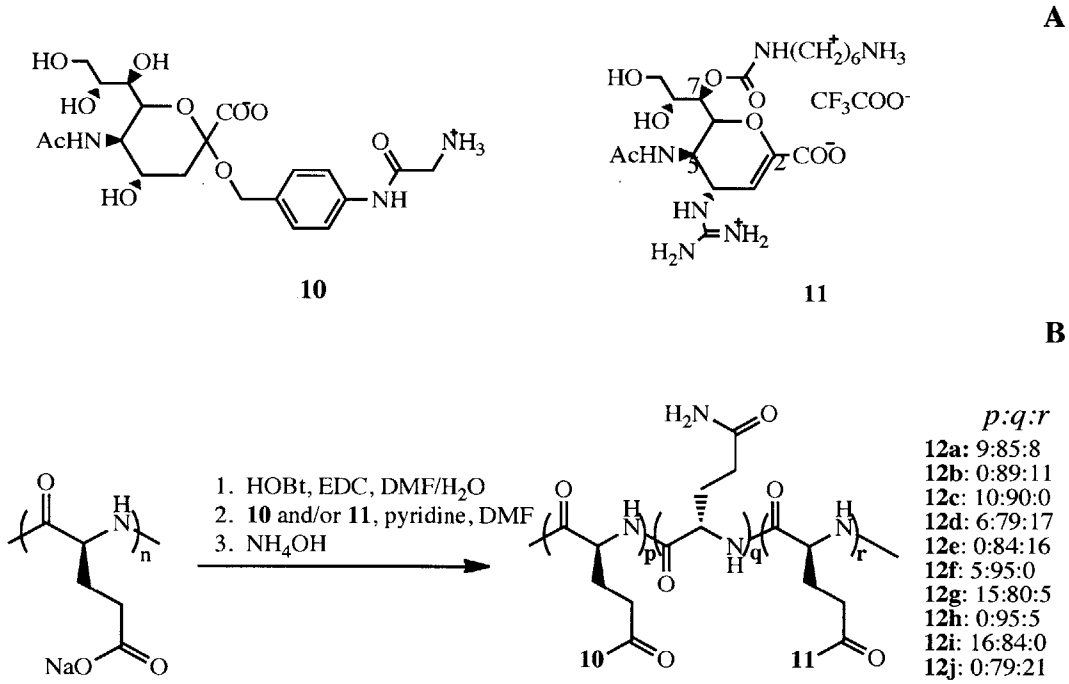

Figure 2-2. Scheme of synthetic route to ZA-derivatized poly-*L*-glutamines. (**A**) α-SA-derivative **10** and ZA-derivative **11** were reacted with (**B**) hydroxybenzotriazole activated poly-*L*-glutamate. The reaction was quenched with ammonium hydroxide to give ZA-derivatized poly-*L*-glutamines (**12a-12j**) with the indicated mole percents of SA (*p*), unmodified side chain (*q*), and/or ZA (*r*). Extent of derivatization was determined by ^{1}H-NMR with an error of ± 2 mole percent.

Next, linker groups were chosen, through which small molecules were conjugated to the polymer backbone. SA was modified at the anomeric carbon which is the only solvent-exposed functional handle. X-ray crystal structures of ZA in the NA active site showed that the 7-OH group is solvent exposed, pointing out and away from the enzyme[30,31]. Masuda *et al.*'s SAR study of derivatives of ZA found that modification of this 7-OH group with alkyl ether substituents less than ten carbon atoms in length (nominally some 16 Å) had no negative effects on antiviral activity compared to ZA itself[23]. Therefore, we initially selected a linker of only six carbon atoms (Fig 2-2 compound **11**). As expected, the introduction of an alkyl carbamate linker group did not drastically affect the anti-viral or NA inhibitory activity; the inhibitory potencies of **11** and ZA were within an order of magnitude of each other (Table 2-1).

Previous efforts showed that inhibition of the H1N1 strain Yamagata was most effective with 10 mole % loading of ZA on poly-*L*-glutamine[23]; other multivalent systems reached a plateau in efficacy between 10% and 30% modification[10,11,32,33]. Thus, we selected 10% loading for our initial experiments as well, and synthesized water-soluble polymeric derivatives of ZA in which the drug was conjugated to poly-*L*-glutamate through a hexyl linker group. The reaction was quenched with ammonium hydroxide[23,26] (Fig 2-2) and conjugation was confirmed and quantified by ^{1}H-NMR. We then assayed the resultant inhibitor using the "gold-standard" viral plaque reduction assay.

Unlike other methods, this cell-based assay directly measures only infectious virions[34,35]. The plaque reduction assay begins with a pre-incubation step of a constant amount of virus with varying amounts of inhibitor. This mixture is used to inoculate a cell monolayer that after infection is covered with a porous agar overlay. As infected cells die, they are trapped by the agar to form an opaque region – a plaque – visible to the eye. Fifty-percent maximal inhibitory concentrations (IC_{50}) were determined from comparison of treated and untreated cells.

Table 2-1. Antiviral activities of ZA (**5**), its monomeric derivative **11**, and poly-*L*-glutamine derivatized with 10 mol % **11** (**12b**), against three influenza A viruses as determined in the plaque reduction assay.

Inhibitor	IC_{50} (nM ZA)[a]		
	WSN (H1N1)	Victoria (H3N2)	Wuhan (H3N2)
ZA	$(5.4 \pm 2.4) \times 10^3$	$(4.8 \pm 1.5) \times 10^4$	$(2.3 \pm 1.6) \times 10^4$
ZA-linker	$(1.0 \pm 0.17) \times 10^3$	$(1.3 \pm 0.32) \times 10^4$	$(4.3 \pm 0.20) \times 10^5$
PGN-ZA	$(1.8 \pm 0.41) \times 10^2$	74 ± 8.5	21 ± 7.3

[a] All values were determined from experiments run at least in triplicate. The IC_{50} values are expressed in concentrations of ZA, whether free or conjugated to poly-L-glutamine. The IC_{50} values for bare poly-L-glutamine ranged from 2 to 8 mM (based on the monomer concentrations) as compared with 0.2 to 40 μM for **12b**, thus demonstrating that the polymer itself has no appreciable antiviral activity. Inhibitors were present during pre-incubation and infection, thus the reported IC_{50} values reflect inhibition of infection. *p*-values were calculated at a 95% confidence interval. There is a statistically significant difference in IC_{50} values between ZA and **11**, and **11** and **12b** for all viruses.

We tested our initial 10%-derivatized inhibitor against three strains of influenza virus: A/WSN/33 (WSN), A/Victoria/3/75 (Victoria), and clinically isolated A/Wuhan/359/95 (Wuhan) (Table 2-1). Against the H1N1 WSN strain we observed a 6-fold reduction in IC_{50} for polymer-attached ZA compared to the small molecule (Table 2-1). Comparably, Masuda *et al* observed a 18-fold reduction for a similar conjugate against the H1N1 Yamagata strain[23]. For the H3N2 strains, however, the observed improvement was orders of magnitude greater: 180-fold and 20,000-fold for Victoria and Wuhan, respectively (Table 2-1).

Next, we investigated whether adding a second, unique pendant group to the polymer backbone affected the inhibitory potency of our original ZA-derivatized poly-*L*-glutamine **12b**. Numerous studies have modified the polymer backbone with groups that had non-specific interactions with the viral surface[10,19,33]. Here, we added SA as a second pendant group with specific binding to HA. Combination therapy, targeting multiple

steps fo the infection cycle, may enhance potency compared to **12b**. We synthesized three bifunctional polymers that did not exceed approximately 20% total derivatization (Fig 2-2) – still within the previously observed optimal efficacy range[10,11,23,32,33] – and tested them against WSN, Victoria, and Wuhan strains. From the results presented in Table 2-2, we can make several important conclusions. First and as expected, when compared to small molecules, bifunctional polymeric inhibitors **12a**, **12d**, and **12g** were far more potent: up to 47,000-fold more than small molecule SA analog **10** and 20,000-fold more than ZA analog **11**. Second, the presence of up to ~15% **11** in a bifunctional polymer enhanced efficacy up to 70-fold compared to the corresponding monofunctional polymers derivatized with SA analog **10**. Third, the presence of up to ~15% **11** in a bifunctional polymer afforded no statistically significant benefits compared to the corresponding monofunctional polymers modified with ZA analog **11**. Fourth, a physical mixture of two monofunctional polymers – one bearing **10** and one **11** – had statistically equivalent potency to the **11**-derivatized component alone.

Table 2-2: Antiviral activities of monomeric derivatives **10** and **11**, and polymeric inhibitors (**12a-12i**) containing varying mole percents of **10**, **11**, or both, against three influenza A viruses as determined in the plaque reduction assay

Inhibitor	% Derivatization[a]		IC_{50} (nM zanamivir)[b]		
	10	**11**	WSN (H1N1)	Victoria (H3N2)	Wuhan (H3N2)
10	N/A	N/A	$>> 10^6$	$>> 10^6$	$>> 10^6$
11[c]	N/A	N/A	$(1.0 \pm 0.17) \times 10^3$	$(1.3 \pm 0.32) \times 10^4$	$(4.3 \pm 0.20) \times 10^5$
12a	9	8	$(1.8 \pm 0.83) \times 10^2$	$(1.4 \pm 0.50) \times 10^2$	30 ± 7.0
12b	0	11	$(1.8 \pm 0.41) \times 10^2$	74 ± 8.5	21 ± 7.3
12c	10	0	$(2.4 \pm 0.21) \times 10^3$	$(3.4 \pm 0.21) \times 10^3$	$(3.0 \pm 0.90) \times 10^2$
12d	6	17	$(2.2 \pm 1.5) \times 10^2$	n.d.	$(1.7 \pm 0.48) \times 10^2$
12e	0	16	$(1.9 \pm 0.92) \times 10^2$	n.d.	$(3.4 \pm 1.0) \times 10^2$
12f	5	0	$(1.6 \pm 0.80) \times 10^4$	n.d.	$(2.8 \pm 1.3) \times 10^3$
12g	15	5	$(1.3 \pm 0.83) \times 10^3$	n.d.	$(1.9 \pm 0.98) \times 10^2$
12h	0	5	$(5.4 \pm 2.1) \times 10^2$	n.d.	$(1.8 \pm 0.50) \times 10^2$
12i	16	0	$(3.5 \pm 0.50) \times 10^3$	n.d.	$(2.4 \pm 0.70) \times 10^2$
12b + 12c	10	11	90 ± 15	n.d.	20 ± 2.1

[a] Percent derivitization with small molecules **10** and **11** was determined by ^{1}H-NMR with an error of ± 2 mole percent.

[b] Inhibitors were present in pre-incubation and infection steps, thus the reported IC_{50} values reflect inhibition of infection. *p*-Values were calculated at a 95% confidence interval. Comparison of all bifunctional inhibitors to their ZA-derivatized monofunctional counterparts demonstrated no statistically signifcant differences in IC_{50}. Comparison of all bifunctional inhibitors to their SA-derivatized monofunctional counterpartes demonstrated statistical significance in all instances except for **12d** against Wuhan strain. Comparison of the physical mixture **12b**+**12c** to **12b** alone showed no statistically significant diference in IC_{50}.

[c] The introduction of a linker group in ZA-derivative **11** did not drastically affect IC_{50} against the avian strain TKY, either.

Previous work in our lab, however, showed that bifunctional PIBMA-based polymeric inhibitors synergistically inhibit Wuhan strain[26], but not other strains (personal communication). The final observations above – that monofunctional inhibitors derivatized with **11** are at least as effective as covalent or physical bifunctional mixtures – both 1) indicated that any previously detected synergism is highly strain- and polymer-dependent and 2) defined the scope of our subsequent studies, which focused on the optimization of monofunctional polypeptides bearing ZA derivatives for inhibition of a

wide range of influenza A viruses.

ZA-derivatized polymers are broad-spectrum inhibitors that overcome drug resistance

In addition to WSN, Victoria, and Wuhan strains, we tested monofunctional polymeric inhibitor **12b** against an avian A/turkey/MN/833/30 (TKY) strain and three drug-resistant strains carrying mutations at position 119: two *in vitro* selected ZA-resistant avian strains TKY E119D and TKY E119G[36] and clinically isolated oseltamivir-resistant Wuhan E119V, which retains transmissibility[37]. Polymeric inhibitor **12b** was 240-fold more potent than **11** against avian strain TKY, extending the trend we observed with human strains (Fig 2-3). Importantly, both oseltamivir- and ZA-resistant mutants were also far more susceptible to polymeric **12b** than to small-molecule inhibitor **11**; we observed a 6000-fold improvement against Wuhan E119V mutant and up to a 2000-fold greater enhancement against zanamivir-resistant TKY mutants (Fig 2-3). Maximal improvements for experimental small molecule inhibitors, however, have not exceeded 1000 times against oseltamivir-resistant influenza strains[38] and 250 times against ZA-resistant ones[39] to date.

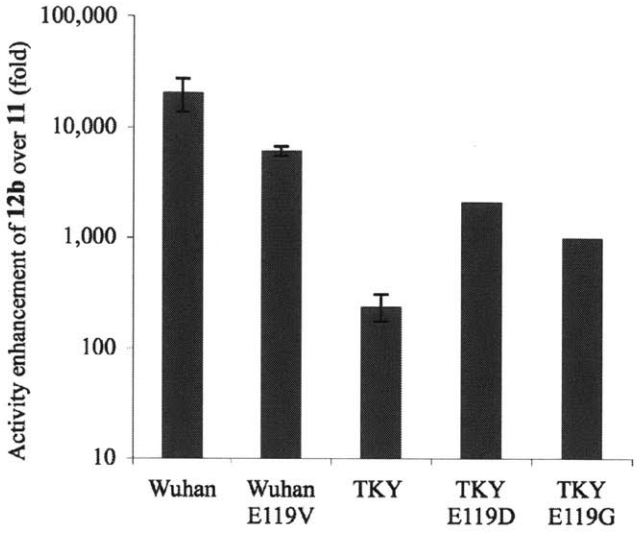

Figure 2-3. Anti-viral activity enhancements of polymeric **12b** over small-molecule **11** against wild-type and drug-resistant influenza strains. ZA-based inhibitors were present during pre-incubation and infection, thus the underlying IC_{50} values reflect inhibition of infection. The reported antiviral activity enhancements reflect experiments run at least in triplicate, except for the TKY mutants which were only run in duplicate due to the large quantities of **11** required. Fifty percent inhibition was not reached for the ZA-resistant mutants, even at millimolar concentrations of **11**; thus the actual enhancements are at least those indicated. Differences in the underlying IC_{50} values are statistically significant with $p < 0.005$.

We expanded our investigation by examining whether the amount of **11** conjugated to poly-*L*-glutamine affects the inhibitory potency of monofunctional inhibitors. Optimal percent conjugation for multivalent systems may differ between previously examined wild-type strains[10,11,23,32,33] and the drug-resistant mutants in which we are interested. Polymeric **12b** (10% of **11**) was up to 16-fold more potent than either **12h** or **12j** (5% and 20%, respectively) against ZA-sensitive strains WSN, Wuhan, Wuhan E119V, and TKY (Fig 2-4). Importantly, **12b** was also up to 8-fold more potent against ZA-resistant TKY strains.

Overall, the observation of the same optimal degree of loading for all the viral strains tested suggests that beyond a certain point, the benefits of multivalency are counteracted by steric effects. Presumably, even when binding affinity is reduced as in

drug-resistant strains, high ligand occupancy interferes with inhibitor binding and/or causes steric clash between ligands that force the polymer into a less active conformation.

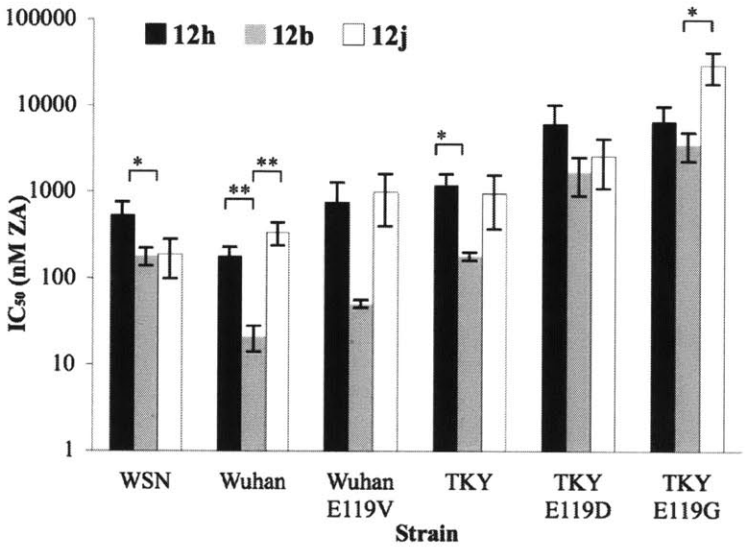

Figure 2-4. Antiviral activities of monofunctional polymers derivatized with 5% (**12h**), 10% (**12b**), or 20% (**12j**) of **11**, against human and avian, drug-susceptible and drug-resistant strains, as determined in the plaque reduction assay. All values were determined from experiments run at least in triplicate. The IC_{50} values are expressed in concentrations of ZA whether free or conjugated to poly-*L*-glutamine. Inhibitors were present during pre-incubation and infection, thus the underlying IC_{50} values reflect inhibition of infection. The IC_{50} values for bare poly-*L*-glutamine ranged from 2 to 10 mM (based on the monomer concentrations), demonstrating that the polymer itself has no appreciable antiviral activity.

We subsequently pursued SAR studies of the linker group and polymer backbone of 10 mole % ZA-polymer conjugates. We examined two alternative linker structures of approximately the same length as our original alkyl linker (10 Å): (i) a flexible and hydrophilic ethylene glycol and (ii) a rigid hydrophobic phenyl (Fig 2-5A, compounds **13** and **14**).

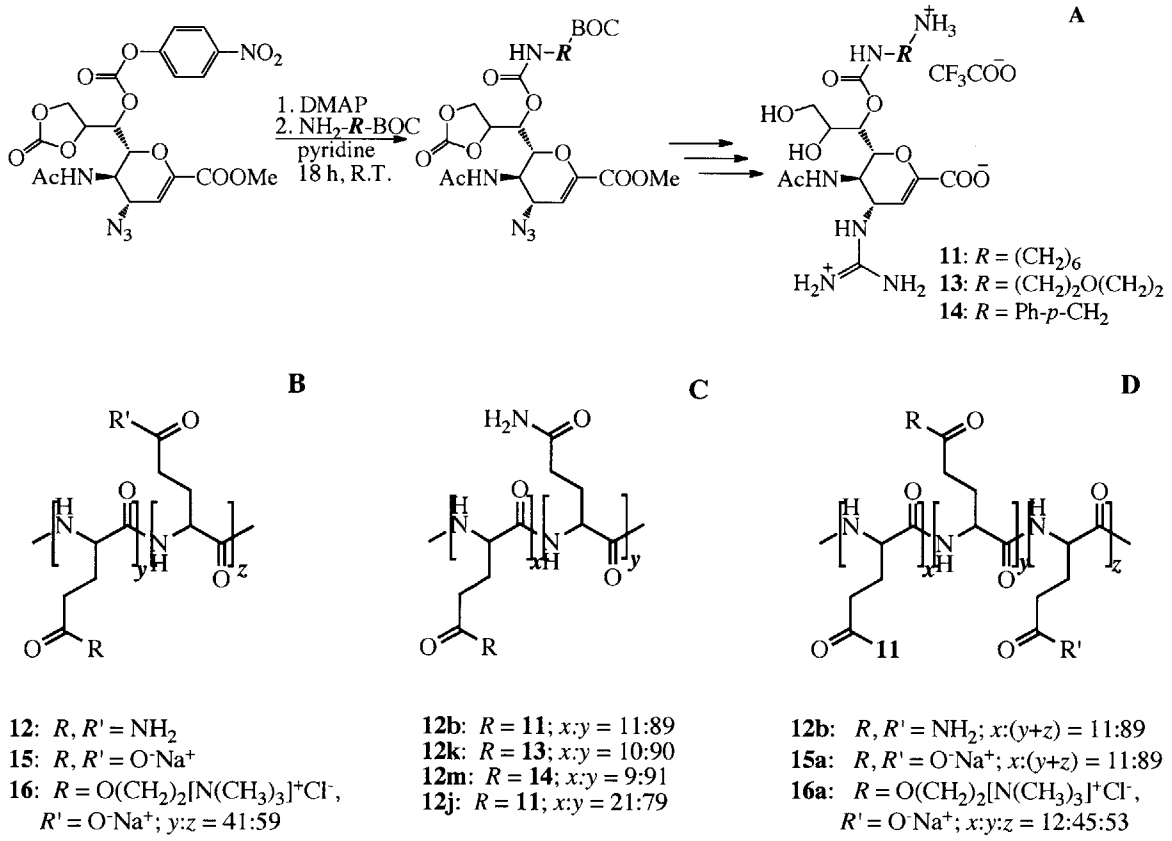

Figure 2-5. (**A**) Synthetic scheme of linker attachment and chemical structures of ZA derivatives with different linkers (**11**, **13**, and **14**) for attachment to (**B**) polymer scaffolds with different electrostatic charges (neutral, negative, and zwitter-ionic) (**12**, **15**, and **16**) to give polymer conjugates with (**C**) varying linker groups (**12b**, **12k**, and **12m**) and (**D**) charges on the polymer backbone (**12b**, **15a**, **16a**).

We tested these ZA analogs in the plaque reduction assay against three strains of influenza virus: WSN, Wuhan, and avian TKY. For all three strains, IC_{50} values showed that **11** was the most potent inhibitor by up to 57-fold over flexible and hydrophilic analog **13** and 76-fold over rigid analog **14** (Fig 2-6). When attached to the poly-*L*-glutamine backbone, compound **12b** - the polymeric conjugate of **11** (Fig 2-5C) – was as good as or better than both **12k** and **12m** (poly-*L*-glutamine conjugates of **13** and **14**, respectively) against WSN and Wuhan viruses, and at least 10-fold more potent against TKY virus (Fig 2-6). Thus we selected ZA analog **11**, which is flexible and moderately

hydrophobic, for subsequent SAR studies of polymer properties. We did not aggressively pursue longer linkers because 1) previous studies by Masuda *et al*[23] showed that 7-*O*-substituents more than ten carbons atoms in length reduced ZA efficacy and 2) ZA binds at the easily accessible head of the NA protein[40], thus only a short linker should be necessary to reach to the binding site. While a longer linker would still increase effective ligand concentration at the viral surface, it may introduce additional steric or entropic costs, potentially counteracting some of the benefit of multivalency.

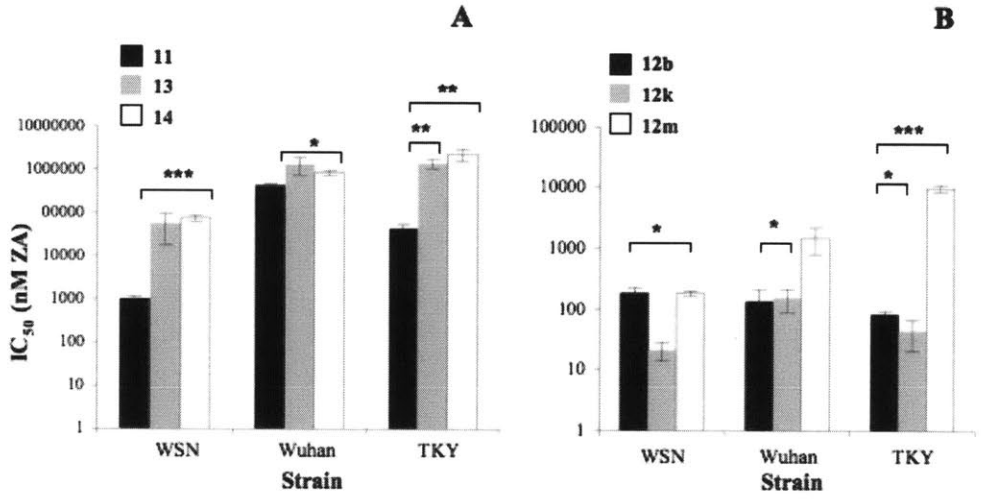

Figure 2-6. Antiviral activities of ZA analogs **11**, **13**, and **14** (**A**), and their polymer-attached derivatives **12b, 12k**, and **12m** (**B**) against three strains of influenza A virus, as determined by the plaque reduction assay. Reported values were determined from experiments run at least in triplicate. IC_{50} values are expressed as concentrations of ZA, whether free or conjugated to polymer. Inhibitor was present during preincubaiton and infection, thus the reported IC_{50} values reflect inhibition of infection. The IC_{50} values for unmodified poly-*L*-glutamine ranged from 2 to 14 mM (on a monomer basis).

Next, we examined the effect of length and charge of the polymer backbone on antiviral activity. Specifically, we used a scaffold of poly-*L*-glutamate of either 3-15 (20-100 repeating units) or 50-100 kDa (330-660 repeating units), and to it conjugated 10 mole percent of **11**. Subsequently, we modified the glutamate side chains with ammonia or choline groups to impart a neutral or zwitter-ionic state, respectively (**15a** and **16a**, Fig

2-5D). We assessed the inhibitory potency of these six polymeric conjugates in the plaque reduction assay with Wuhan, TKY, and ZA-resistant TKY E119D strains. Conjugate **16a**, regardless of molecular weight or virus strain, had the highest IC_{50} value (Fig 2-7). For negatively charged conjugate **15a**, the low molecular weight inhibitor had an IC_{50} up to 4-fold lower than the high molecular weight conjugate. Conversely, high molecular weight **12b** was up 15-fold more potent than the low molecular weight variant against all three viruses, and up to 75-fold more potent compared to corresponding charged analogs **15a** and **16a** (Fig 2-7). Also, polymer structure did not have a greater effect on IC_{50} when binding of **11** is weaker (i.e., for TKY E119D strain).

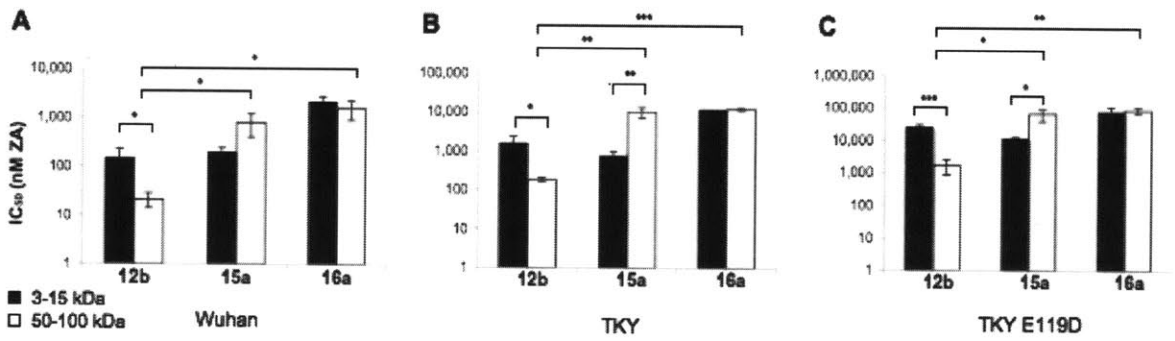

Figure 2-7. IC_{50} values for low-molecular-weight (3-15 kDa; black bars) and high-molecular-weight (50-100 kDa; white bars) conjugates **12b**, **15a**, and **16a** against (**A**) Wuhan, (**B**) TKY, and (**C**) TKY E119D isolates of influenza A virus. IC_{50} values, reported as nanomolar concentrations of ZA, were determined using the plaque reduction assay with inhibitor present during preincubation and infection. Thus, IC_{50} values reflect inhibition of infection. IC_{50} values of bare backbones **12**, **15**, and **16** ranged from 2 to 39 mM, compared to at least 85 μM for drug conjugates. Thus, the polymers themselves had no appreciable antiviral activity. * $p < 0.05$, ** $p < 0.01$, and *** $p < 0.001$ were determined by a two-tailed Student's *t*-test. All reported values are the mean ± SD of at least three independent measurements.

In their study of sialic acid-derivatized polyacrylamides that bind the HA of influenza virus, the Whitesides group reported that addition of charge to the backbone – either positive or negative – decreased binding strength in an erythrocyte sedimentation assay[9,10]. Our results suggest that the same trend applies to NA-binding poly-*L*-

glutamate-based conjugates of **11** in the plaque reduction assay. Changes in polymer conformation due to the addition of charge[10] would be particularly relevant with peptide-based scaffolds and could affect the ability of the drug conjugate to inhibit viral infection.

Mechanisms of multivalent inhibition

To gain further quantitative mechanistic insights, we determined inhibition constants K_i for both **11** and **12b**, using drug-resistant strains and the corresponding wild-type Wuhan and TKY viruses in a whole-virus NA inhibition assay. There are several important conclusions gleaned from the data presented in Table 2-3. First, **11** binds at least two orders of magnitude weaker to ZA-resistant strain TKY E119D and E119G (last two lines of Table 2-3) than to the wild-type and oseltamivir-resistant strains. This is in good agreement with the original literature report on these strains[36]. Second, ZA-derivatized **12b** is a substantially more potent enzyme inhibitor than small molecule ZA. Third, while binding affinity enhancements resulting from polymer conjugation are relatively modest for wild-type and oseltamivir-resistant strains, ZA-resistant TKY mutants bind **12b** 2000 times stronger than **11**. Because of this strengthened binding, the ZA-resistant mutants become as sensitive to **12b** (in contrast to **11**) as the other strains (Table 2-3). Presentation of ZA on the polymer entirely compensates for weakened binding in ZA-resistant TKY strains.

Table 2-3. Inhibition constants (*Ki*) of viral NAs by small-molecule (**11**) and polymeric (**12b**) ZA derivatives against both wild-type and drug-resistant human and avian influenza A strains.

Strain	*Ki* (nM ZA)[a,b]	
	11	**12b**
Wuhan	3.1 ± 1.0	0.93 ± 0.12
Wuhan E119V	1.9 ± 0.81	0.90 ± 0.10
TKY	4.6 ± 0.92	0.27 ± 0.16
TKY E119D	800 ± 150	0.37 ± 0.12
TKY E119G	370 ± 20	0.13 ± 0.054

[a] All values were determined from experiments run at least in triplicate. The *Ki* values are expressed in concentrations of ZA, whether free or conjugated to poly-*L*-glutamine. Even at 10 mM, bare poly-*L*-glutamine showed no inhibition of NA activity, thus the polymer itself has no appreciable enzyme inhibitory activity. For conditions, see Materials and Methods.

[b] Enhancement of **12b** over **11** is statistically significant for all strains except Wuhan E119V (p=0.0508).

Multivalent drug species, such as **12b**, tend to exhibit better virus inhibition as a result of entropic and steric effects, and increased affinity[8,10,41]. There should be similar rotational and translational entropic costs for the initial interaction with viral surface proteins for both free and polymer-bound ZA. Polymer-bound ZA, however, should have lower costs for subsequent interactions, thereby providing entropic benefits of multivalency[41]. Flexible linkers and polymers such as that employed so far in this study, can promote improved ligand–protein binding by reducing steric obstacles and increasing effective ligand concentration[42] (as is schematically illustrated in Figure 2-1).

Surprisingly, however, our lab has shown that **12b** has an additional synergistic mechanism of action that enhances eficacy: inhibition of early intracellular stages of infection[43]. Specifically, in the presence of **12b** but not ZA, we saw 1) an accumulation of endocytosed virions co-localized with cellular acidic compartments and 2) an inhibition of HA fusion with cell membranes at fusion-inducing low pH[43]. These observations suggested that **12b** interferes with trafficking and HA-mediated virus-

endosome fusion.

Previously, we observed no significant strain or subtype specificity for the interaction of **12b** with viral NAs as would occur during viral budding and aggregation (Table 2-3). Next, we sought to determine if **12b** inhibitory activity was strain or subtype specific in either the early stages or across all stages of infection (including but not limited to inhibition of NA activity). To this point, inhibitor has been present in the plaque assay during pre-incubation and infection, inhibiting only early events such virus-endosome fusion (-1-1 h) (Fig 2-8). Additionally, here we added ZA or **12b** to the agar overlay to examine for inhibition of virion release and multicycle infection as well (-1-72 h).

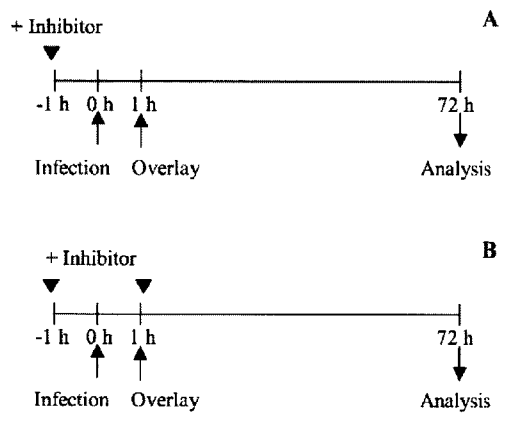

Figure 2-8. Experimental design for the plaque reduction assay of inhibition at (**A**) early stages (-1 - 1 h) of infection and (**B**) throughout (-1 - 72 h) infection. Inhibitor is added to a virus solution and pre-incubated for 1 h. After infection, the virus and inhibitor mixture is removed and an agarose overlay containing (**A**) PBS or (**B**) inhibitor is placed on the cells. Analysis of plaque number is performed at 72 h.

As expected for ZA – whose only mechanism of action is direct inhibition of late-stage NA activity – inclusion in the agar enhanced IC_{50} at least 100-fold for all strains (Table 2-4). For **12b** against H3N2 strains, we saw at most a 3-fold improvement in IC_{50} (Table 2-4) compared to values for only the initial stages of infection. For H1N1 and H4N2 strains, however, we saw up to a 72- and greater than 180-fold enhancement in efficacy, respectively, when inhibitor **12b** was present during all stages of the infection

cycle. This suggests that **12b** has a greater effect on virus-endosome fusion in H3N2 strains, perhaps because H3N2 viruses have a more pH-sensitive HA fusion process. These results underscore the need to study many strains of influenza virus.

Table 2-4. IC_{50} values for inhibition of influenza A viruses in the plaque reduction assay by ZA and polymer **12b** during all stages . The polymeric inhibitor was included during pre-incubation and infection steps of the assay. **12b** was either absent (-1-1 h) or present (-1-72 h) in the agar overlay to assay for early stage infection or multi-cycle infection, respectively.

Strain	Subtype	IC_{50} (nM zanamivir)[a]			
		Polymeric **12b**		Small molecule **11**	
		-1-1 h (early stages)	-1-72 h (all stages)	-1-1 h (early stages)	-1-72 h (all stages)
Wuhan	H3N2	21 ± 7.3	8.7 ± 0.70	(4.3 ± 0.20) x 10^5	(3.6 ± 0.45) x 10^2
Wuhan E119V		51 ± 5.0	17 ± 6.2	(3.1 ± 0.10) x 10^5	(2.2 ± 1.7) x 10^2
Victoria		74 ± 8.5	30 ± 8.0	(1.3 ± 0.32) x 10^4	(2.6 ± 0.47) x 10^3
WSN	H1N1	(1.8 ± 0.41) x 10^2	2.5 ± 1.0[b]	(1.0 ± 0.17) x 10^3	58 ± 11[b]
PR8		(3.0 ± 0.89) x 10^2	1.7 ± 1.2	(4.5 ± 1.5) x 10^3	(8.8 ± 0.20) x 10^2
TKY	H4N2	(1.8 ± 0.20) x 10^2	2.1 ± 0.44	(4.3 ± 1.1) x 10^4	(2.5 ± 0.12) x 10^2
TKY E119D		(1.7 ± 0.83) x 10^3	34 ± 16	>3.6 x 10^6	(2.2 ± 1.1) x 10^4
TKY E119G		(3.6 ± 1.3) x 10^3	20 ± 4.9	>3.6 x 10^6	(7.1 ± 0.14) x 10^4

[a] Reported values are the average of triplicate measurements unless otherwise indicated. Horizontal lines within the table separate subtypes. There is a statistically significant difference between IC_{50} values obtained at -1-1 h and -1-72 h for both **11** and **12b** against all strains, with p-values ranging from 0.0001 to 0.0479.

[b] Reported IC_{50} value is the average of two measurements.

Conclusion

Overall, conjugate **12b** with its long, neutral backbone and short, flexible linker is the most potent inhibitor of the derivatives examined herein. We have also demonstrated broad-spectrum efficacy and a noteworthy ability of **12b** to overcome drug resistance by enhancing ZA binding strength. *In vitro* efficacy, however, does not always translate to animal models of disease. In Chapter 3, we examine efficacy and immunogenicity of conjugate **12b** in the mouse and ferret models of influenza infection.

Acknowledgements

I would like to thank Dr. Chia Min (Jaimie) Lee and Alyssa Larson for their efforts to help maintain our cell line. I appreciate Dr. Chia Min Lee's willingness to do help make virus stocks as necessary. Also, I am grateful to Dr. Meredith Hartley and Dr. Angelyn Larkin for taking the time to review this chapter, and their thoughtful and thorough comments.

C. MATERIALS AND METHODS

Chemicals

Poly-*L*-glutamic acid sodium salt (molecular weight = 3,000 – 15,000 and 50,000– 100,000 Da) and all other chemicals and solvents were purchased from Sigma-Aldrich Chemical Co (St. Louis, Missouri, USA) unless otherwise indicated.

Synthesis and characterization

ZA was obtained from BioDuro (Beijing, China). ZA derivative **11** (Fig 2-2) was synthesized from combined literature procedures[44,45] as described previously[26]. Sialic acid derivative **10** (Fig 2-2) was prepared from combined literature procedures[46-48] as described previously[26], except for linker attachment in which silver zeolite was used in place of mercury salts (see **18** below). Polymer conjugates **12a-12j** were prepared using a modified literature procedure[22] (Fig 2-2). Bare poly-*L*-glutamine (**12**) was synthesized analogously. All intermediates and target derivatives were analyzed by ^{1}H-NMR. Content of SA and ZA in polymeric inhibitors was quantified by ^{1}H-NMR.

***Methyl-2-(4*-tert-butoxycarbonylglycylamidobenzyl)-5-acetamido-4,7,8,9-tetra-*O*-acetyl-3,5-dideoxy-2-oxo-D-*glycero*-D-*galacto*-2-nonulopyranosonate** (**18**, an intermediate in the synthesis of **10**; Fig 2-9) was synthesized using a combination of literature procedures[49-51]. To a reaction vessel protected from light were added solid chlorinated sialic acid (0.1 mmol, (1-(3-acetamido-4-acetoxy-6-chloro-6-(methoxycarbonyl)tetrahydro-2*H*-pyran-2-yl)propane-1,2,3-triyl triacetate)), (4-*tert*-butoxycarbonylglycylamido)benzyl alcohol[48] (0.048 mmol), powdered 4Å molecular

sieves, and 35% silver zeolite freshly prepared as previously described[52] and dried overnight under nitrogen at 150°C. The vessel was purged and CH_2Cl_2 (10 mL) was added. The mixture was vigorously stirred under nitrogen at RT for 30 hours. After diluting with DCM (10 mL) the mixture was filtered through a celite pad and solvent was evaporated. Purification on a silica gel (230-400 mesh) column with EtOAc:Toluene 1:1 yielded the title compound in 20% yield (overall yield for both anomers was very high at 70%).

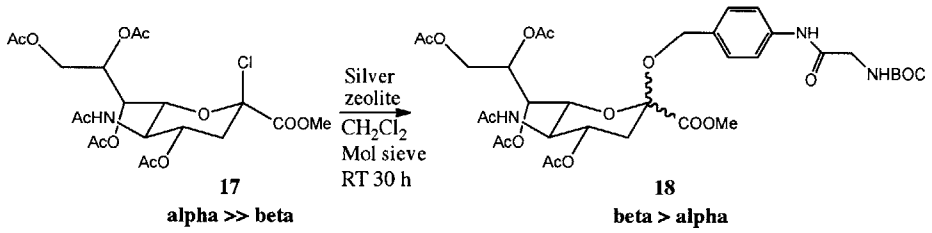

Figure 2-9. Reaction scheme for silver-mediated linker attachment to chlorinated sialic acid. SA chlorination with HCl produces mostly the α-anomer (**17**). A subsequent Koenigs-Knorr-type reaction results largely in inversion at the glycosidic bond (**18**). The α-anomer of **18** is produced because there is no ester on the adjacent carbon to act as an intramolecular nucleophile and promote 100% inversion.

^{1}H-NMR ($CDCl_3$) δ (400 MHz) – 1.40 (9H, s, $C(CH_3)_3$), 1.85 (4H, m, $NCOCH_3$, H-3_{ax}), 2.0 (3H, s, $OCOCH_3$), 2.15 (6H, s, 2 x $OCOCH_3$), 2.70 (1H, dd, H-3_{eq}), 3.55 (3H, s, OCH_3), 3.80 (1H, dd, H-6), 3.85-4.00 (4H, m, OCH_2, $COCH_2NH$), 4.05-4.15 (2H, m, H-9_a, H-5), 4.33 (1H, dd, H-9_b), 4.70 (1H, ddd, H-4), 5.30 (1H, dd, H-7), 5.35-5.45 (1H, m, H-8), 5.70 (1H, d, $NHCOCH_3$), 7.20 and 7.35 (4H, 2d, aromatic).

3-Acetamido-2-(1-(((2-(2-aminoethoxy)ethyl)carbamoyl)oxy)-2,3-dihydroxypropyl)-4-guanidino-3,4-dihydro-2H-pyran-6-carboxylic acid (13) was synthesized using a modified literature procedure[44,45] with *tert*-butyl-(2-(2-aminoethoxy)ethyl)carbamate (ChemPep, Wellington, FL) to introduce the linking group. Subsequent

reduction/deprotection with triphenyl phospine/triethylamine/H_2O and guanidinylation with *N,N'*-bis-*t*-butoxycarbonyl-1H-pyrazole-1-carboxamidine of intermediates were performed as previously described[44,45], with modification to the purification schemes. For both intermediates, purification was done using a reverse-phase silica plug (Sep Pak C18 cartridge vac 6cc, Water, Milford, MA). Intermediates were loaded in water and 1:4 H_2O:methanol, respectively. Product was eluted with 12 mL of water followed by either 15% acetonitrile or 40% methanol, respectively. BOC-deprotection was performed as previously described[44,45] to give compound **5**. ^{1}H NMR (D_2O) δ (500 MHz) – 1.85 (3H, s, CH_3CONH), 3.05-3.25 (4H, m, -NHCH$_2$$CH_2OCH_2CH_2NH_2$), 3.40 (1H, dd, H-9$_a$), 3.50 (2H, m, -NH$CH_2CH_2OCH_2CH_2NH_2$), 3.60 (1H, d, H-9$_b$), 3.65 (2H, m, -NHCH$_2CH_2OCH_2$$CH_2NH_2$), 3.95 (1H, m, H-8), 4.05 (1H, t, H-5), 4.35 (1H, d, H-4), 4.45 (1H, d, H-6), 4.90 (1H, d, H-7), 5.95 (1H, d, H-3).

3-Acetamido-2-(1-(((4-(aminomethyl)phenyl)carbamoyl)oxy)-2,3-dihydroxypropyl)-4-guanidino-3,4-dihydro-2H-pyran-6-carboxylic acid (14) was synthesized analogously to **13** above using *tert*-butyl-4-aminobenzylcarbamate to introduce the linker group. ^{1}H NMR (D_2O) δ (500 MHz) – 1.85 (3H, s, CH_3CONH), 3.45 (1H, q, H-9$_a$), 3.60 (1H, d, H-9$_b$), 4.10-4.20 (2H, m, H-5 and H-8), 4.35-4.45 (3H, m, PhCH_2NH$_2$ and H-4), 4.50 (1H, d, H-6), 5.0 (1H, d, H-7), 5.85 (1H, d, H-3), 7.25-7.35 (4H, m, aromatic).

Polymer conjugates 12k and 12m were synthesized analogously to **12b**[22]. ^{1}H NMR (D_2O) δ (500 MHz) – for **12k**: 1.8-2.1 (5H, m, 2H polymer and CH_3CONH), 2.1-2.4 (2H, d, 2H polymer), 3.0-3.2 (4H, m, NHCH$_2$$CH_2OCH_2CH_2NH_2$), 3.35-3.45 (2H, m, NH$CH_2CH_2OCH_2CH_2NH_2$), 3.45 (1H, dd, H-9$_b$), 3.55 (1H, d, H-9$_a$), 3.6 (2H, m, NHCH$_2CH_2OCH_2$$CH_2NH_2$), 3.95 (1H, m, H-8), 4.05-4.25 (2H, s, 1H polymer and H-5),

4.45 (1H, d, H-4), 4.55 (1H, d, H-6), 5.7 (1H, s, H-3). For **12m**: 1.9-2.1 (5H, m, 2H polymer and CH_3CONH), 2.2-2.4 (2H, d, 2H polymer), 3.5 (1H, q, H-9_a), 3.6 (1H, dd, H-9_b), 4.1-4.35 (9H, m, 4H polymer, H-4, H-5, H-8, PhCH_2NH_2), 4.5 (1H, d, H-6), 5.7 (1H, d, H-3), 7.3 (4H, m, 4H aromatic)

Conjugate 15a and scaffold 15. Conjugate **15a** was synthesized analogously to **12b**[22] using 3 mL of 0.1 M NaOH to quench the polymer conjugation reaction for 48 h at RT. Un-derivatized **15** was synthesized by quenching benzotriazole-activated poly-*L*-glutamate with an excess of 0.1 M NaOH. After quenching, both reactions were diluted with distilled water and buffer exchanged into the same at least four times using an Amicon Ultra Centrifugal Filter with an Ultracel regenerated cellulose membrane (15 mL, 15 kDa MWCO) at 4,000 x *g* before lyophilization. ^{1}H NMR (D_2O) δ (500 MHz) – For **15a**: 1.1-1.4 (8H, m, -NHCH$_2$(CH_2)$_4$$CH_2NH_2$), 1.7-2.4 (7H, m, 4H polymer and CH_3CONH), 2.8-3.05 (4H, m, -NHCH_2(CH_2)$_4$$CH_2NH_2$), 3.5 (1H, dd, H-$9_b$), 3.6 (1H, d, H-$9_a$), 3.8 (2H, m, H-5, H-8), 4.1-4.25 (1H, s, 1H polymer), 4.45 (1H, d, ZA), 4.55 (1H, d, H-6), 5.0 (1H, d, H-7), 5.75 (1H, s, H-3). For **15**: 1.7-2.3 (4H, m, 4H polymer), 4.2 (1H, s, 1H polymer).

Conjugate 16a and scaffold 16. Attachment of **11** to the activated polymer scaffold was performed analogously to **12b**[22]. After 4 h, the reaction was cooled on an ice bath. Solid *N*-ethyl-*N*'-(3-dimethylaminopropyl)carbodiimide hydrochloride (2.72 mg, 0.0142 mmol, 1.2 equiv) was added to the reaction mixture, which was subsequently purged with argon gas. A solution of 4-dimethylaminopyridine (0.072 mg, 0.00059 mmol, 0.05 eq) in DMF (15 μL) was then added, and the mixture stirred for 5 min. A pre-cooled solution of choline chloride (6.59 mg, 0.0472 mmol, 4 equiv) in formamide (240 μL to give a final

concentration of formamide in reaction of 30% v/v) was then added dropwise. The reaction was stirred on ice for 16 h and allowed to warm to RT overnight. Bare **16** was synthesized by quenching benzotriazole-activated poly-*L*-glutamate with choline chloride in formamide as described above. After quenching, both reactions were diluted with distilled water and buffer exchanged into the same at least four times using an Amicon Ultra Centrifugal Filter with a regenerated cellulose membrane (15 mL, 15 kDa MWCO) at 4,000 x *g* before lyophilization. ^{1}H NMR (D_2O) δ (500 MHz) – For **16a**: 1.2-1.5 (8H, m, -NHCH$_2$*(CH$_2$)$_4$*CH$_2$NH$_2$), 2.0-2.8 (7H, m, 4H polymer and *CH$_3$*CONH), 2.9-3.05 (4H, m, -NH*CH$_2$*(CH$_2$)$_4$*CH$_2$*NH$_2$), 3.2 (9H, s, -N(*CH$_3$*)$_3$), 3.5 (1H, dd, H-9$_a$), 3.55 (1H, d, H-9$_b$), 3.7 (2H, s, -*CH$_2$*N-) 4.05 (2H, m, H-8 and H-5), 4.1-4.3 (2H, 1H polymer and H-4), 4.5 (1H, d, H-6), 4.55 (2H, s, -*CH$_2$*O-), 5.65 (1H, s, H-3). For **16**: 2.0-2.8 (4H, m, 4H polymer), 3.25 (9H, s, -N(*CH$_3$*)$_3$), 3.8 (2H, s, -*CH$_2$*N-), 4.15-4.4 (1H, s, 1H polymer), 4.65 (2H, s, *CH$_2$*O-).

Influenza Virus

Plaque-purified influenza A/WSN/33 (WSN; H1N1) and A/Victoria/3/75 (Victoria; H3N2) were cultured in E4HG medium from MDCK cells (ATCC; Manassas, VA) for 2-3 days, clarified, and filtered through a 0.2-μm filter to remove aggregates. Influenza virus strains A/Wuhan/359/95 (Wuhan; H3N2), A/turkey/MN/833/80 (TKY; H4N2), and A/turkey/MN/833/80/E119D drug-resistant mutant (TKY E119D) were obtained from the Centers for Disease Control and Prevention (Atlanta, GA), and propagated as previously described[26]. Sucrose-gradient purified influenza A/PR/8/34 (PR8; H1N1) was obtained from Charles River Labs in HEPES-saline buffer (Wilmington, MA) and diluted with PBS (pH 7.2) before use. Titers were determined by serial titration in the plaque assay[53]. Stocks of influenza A/Nanchang/933/95 (Nanchang)

H3N2 virus were grown in the allantoic cavities of 10-day-old embryonated hens' eggs at 34°C for 48-72 h. Pooled allantoic fluid was clarified by centrifugation and stored at -70°C.

Plaque Reduction Assay

Plaque assays were performed in 12-well plates using a modified literature procedure[26,34]. For the pre-incubation step, 55 μL of virus diluted in PBS (~800 pfu/mL) was incubated with an equal volume of inhibitor solution in PBS (serially 10-fold diluted) for 1 h at room temperature. After washing, confluent MDCK cell monolayers were infected at room temperature for 1 h with 100 μL of the virus–inhibitor mixture. The inoculum was removed by aspiration, and the cells were overlaid with 1 mL of plaque medium [2X F12 medium, 0.01% DEAE-dextran, 0.1% $NaHCO_3$, 100 units/mL of penicillin G, 100 μg/mL of streptomycin, 4 μg/mL of trypsin, and 0.6% purified agar (L28; Oxoid Co., Basingstoke, UK)]. Plaques were counted after 3 to 4 days of incubation at 37◦ C.

Neuraminidase Inhibition Assay

Neuraminidase inhibition assays were performed using a modified literature procedure[54]. Briefly, whole virus (20 μL) and inhibitor dilutions (15 μL) were incubated at room temperature for 1 h. Following addition of fluorogenic substrate 4-methylumbelliferyl-α-D-*N*-acetylneuraminic acid (final concentration of 2 μM was 5- to 10-fold lower than the K_m of the enzymes), generation of 4-methylumbelliferone was monitored at 5 min intervals for 1 h. Substrate fluorescence was inhibitor dose-dependent. Values of *K*i were determined using nonlinear regression[55] in KaleidaGraph.

Statistical Analysis

Unpaired two-tailed Student's *t*-test was performed using Prism 6 software at 95% confidence interval.

D. References

1. World Health Organization, Weekly epidemiological record. 4 November **2011**, 45, (86), 497-508.
2. Thorlund K, Awad T, Boivin G, Thabane L, Systematic review of influenza resistance to the neuraminidase inhibitors. *BMC Infect Dis*, **2011**, 11, 134.
3. Administration USFaD, FDA authorized emergency use of intravenous antiviral peramivir for 2009 H1N1 influenza for certain patients, settings. **2009**, U.S. Food and Drug Administration, FDA NOTE TO CORRESPONDENTS. http://www.fda.gov/downloads/Drugs/DrugSafety/PostmarketDrugSafetyInformationforPatientsandProviders/UCM187811.pdf
4. Belser J, Lu X, Szretter KJ, Jin X, Aschenbrenner LM, Lee A, Hawley S, Kim do H, Malakhov MP, Yu M, Fang F, Katz JM, DAS181, A novel sialidase fusion protein protects mice from lethal avian influenza H5N1 infection, *Infect Dis*, **2007**, 196, (10), 1493-1499.
5. Triana-Baltzer GB, Gubareva LV, Nicholls JM, Pearce MB, Mishin VP, Belser JA, Chen LM, Chan RW, Chan MC, Hedlund M, Larson JL, Moss RB, Katz JM, Tumpey TM, Fang G, Novel pandemic influenza A (H1N1) viruses are potently inhibited by DAS181, a sialidase fusion protein. *PloS One*, **2009**, 4, (1), e7788
6. Triana-Baltzer GB, Gubareva LV, Klimov AI, Wurtman DF, Moss RB, Hedlund M, Larson JL, Belshe RB, Fan F, Inhibition of neuraminidase inhibitor-resistant influenza virus by DAS181, a novel sialidase fusion protein. *PloS One*, **2009**, 4, (11), e7838.
7. Moss RB, Davey RT, Steigbigel RT, Fang F, Targeting pandemic influenza: a primer on influenza antivirals and drug resistance. *J Antimicrob Chemother*, **2010**, 65, (6), 1086-1093.
8. Mammen M, Choi S-K, Whitesides GM, Polyvalent interactions in biological systems: Implications for design and use of multivalent ligands and inhibitors. *Angew Chem Int Ed,* **1998**, 37, 2754–2794.
9. Sigal GB, Mammen M, Dahmann G, Whitesides, Polyacrylamides bearing pendant α-sialoside groups strongly inhibit agglutination of erythrocytes by influenza virus: the strong inhibition reflects enhanced binding through cooperative polyvalent interactions. *J Am Chem Soc*, **1996**, 118,3789-3800.
10. Mammen M, Dahmann G, Whitesides GM, Effective inhibitors of hemagglutination by influenza virus synthesized from polymers having active ester groups. *J Med Chem*, 38, 4179–4190.
11. Matrosovich MN, Mochalova LV, Marinina VP, Byramova NE, Bovin NV, Synthetic polymeric sialoside inhibitors of influenza virus receptor-binding activity. *FEBS Lett*, **1990**, 272, (1,2), 209-212.
12. Gambaryan AS, Boravleva EY, Matrosovich TY, Matrosovich MN, Klenk H-D, Moiseeva EV, Tuzikov AB, Chinarev AA, Pazynina GV, Bovin NV, Polymer-bound 6' sialyl-*N*-acetyllactosamine protects mice infected by influenza virus. *Antiviral Res*, **2005**, 68, 116-123.
13. Lees WH, Spaltenstein A, Kingery-Wood JE, Whitesides GM, Polyacrylamides Bearing Pendant α-Sialoside Groups Strongly Inhibit Agglutination of Erythrocytes by Influenza A Virus: Multivalency and Steric Stabilization of Particulate Biological Systems. *J Med Chem*, **1994**, 36, 3419-3433.

14. Mochalova LV, Tuzikov AB, Marinina VP, Gambaryan AS, Byramova NE, Bovin NV, Matrosovich MN, Synthetic polymeric inhibitors of influenza virus receptor-binding activity suppress virus replication. *Antiviral Res*, **1994**, 23, 179-190.
15. Tsuchida A, Kobayashi K, Matsubara N, Muramatsu T, Suzuki T, Suzuki Y, Simple synthesis of sialyllactose-carrying polystyrene and its binding with influenza virus. *Glycoconj J*, **1998**, 15, 1047-1054.
16. King DJ, Noss RR, Toxicity of polyacrylamide and acrylamide monomer. *Rev Environ Health*, **1989**, 8:3-16.
17. Xi TF, Fan CX, Feng XM, Wan ZY, Wang CR, Chou LL, Cytotoxicity and altered c-myc gene expression by medical polyacrylamide hydrogel. *J Biomed. Mat Res*, **2006**, 78A, 283-290.
18. Totani K, Kubota T, Kuroda T, Muarata T, Hidari KI-P, Suzuki T, Suzuki Y, Kobayashi K, Ashida H, Yamamoto K, Usui T, Chemoenzymatic synthesis and application of glycopolymers containing multivalent sialyloligosaccharides with a poly(L-glutamic acid) backbone for inhibition of infection by influenza viruses. *Glycobiol*, **2003**, 13, 315-326.
19. Reuter JD, Myc A, Hayes MM, Gan Z, Roy R, Qin D, Yin R, Piehler LT, Esfand R, Tomalia DA, Baker JR Jr, Inhibition of Viral Adhesion and Infection by Sialic-Acid-Conjugated Dendritic Polymers. *Bioconj Chem*, **1999,** 10, 271-278.
20. Roy R, Pon RA, Tropper RD, Andersson FO, Michael addition of poly-L-lysine to *N*-acryloylated sialosides. Syntheses of influenza A virus haemagglutinin inhibitor and group B meningococcal polysaccharides vaccines. *J Chem Soc Chem Commun*, **1993**, 3, 264-265.
21. Kamitakahara H, Suzukoi T, Nishigori N, Suzuki Y, Kanie O, Wong C-H, A Lysoganglioside/Poly-L-glutamic Acid Conjugate as a Picomolar Inhibitor of Influenza Hemagglutinin. *Angew Chem Int Ed*, **1998**, 37, (11), 1524-1528.
22. Honda T, Yoshida S, Arai M, Masuda T, Yamashita M, Synthesis and anti-influenza evaluation of polyvalent sialidase inhibitors bearing 4-guanidino-Neu5Ac2en derivatives. *Bioorg Med Chem Lett*, **2002**, 12, 1929-1932.
23. Masuda T, Yoshida S, Arai M, Kaneko S, Yamashita M, Honda T, Synthesis and anti-influenza evaluation of polyvalent sialidase inhibitors bearing 4-guanidino-Neu5Ac2en derivatives. *Chem Pharm Bull*, **2003**, 51, 1386–1398.
24. Reece, PA, U.S. Patent 6,680,054, **2004**.
25. Rathbun RC, Lockhart S, Stephens JR, Current HIV treatment guidelines--an overview. *Curr Pharm Des,* 12, 1045-1063.
26. Haldar J, Alvarez de Cienfuegos L, Tumpey TM, Gubareva LV, Chen J, Klibanov AM. Bifunctional polymeric inhibitors of human influenza A viruses. *Pharm Res*, **2010**, 27, 259–263.
27. Nissen TL, Andersen KV, Hansen CK, Mielsen JM, Schambye HT, U.S. Patent Application 20060084793, **2006**.
28. Chipman SD, Oldham FB, Pezzoni G, Singer JW, Biological and clinical characterization of paclitaxel poliglumex (PPX, CT-2103), a macromolecular polymer-drug conjugate. *Int J Nanomedicine*, **2006,** 1, (4), 375–383.
29. Homsi J, Simon GR, Garrett CR, Springett G, De Conti R, Chiappori AA, Munster PN, Burton MK, Stromatt S, Allievi C, Angiuli P, Eisenfeld A, Sullivan

DM, Daud AI, Phase I Trial of Poly-L-Glutamate Camptothecin (CT-2106) Administered Weekly in Patients with Advanced Solid Malignancies. *Clin Cancer Res*, **2007**, 13, 5855-5861.

30. Varghese JN, Epa VC, Colman PM, Three-dimensional structure of the complex of 4-guanidino-Neu5Ac2en and influenza virus neuraminidase. *Protein Sci*, **1995**, 4, 1081-1087.
31. Colman PM, Varghese JN, Laver WG, Structure of the catalytic and antigenic sites in influenza virus neuraminidase. *Nature*, **1983**, 303, 41-44.
32. Spevak W, Nagy JO, Charych DH, Schaefer ME, Gilbert JH, Bednarski MD, Polymerized liposome containing *C*-glycosides of sialic acid: potent inhibitors of influenza virus in vitro infectivity. *J Am Chem Soc*, **1993**, 115, 1146-1147
33. Spaltenstein A, Whitesides GM, Polyacrylamides bearing pendant alpha-sialoside groups strongly inhibit agglutination of erythrocytes by influenza virus. *J Am Chem Soc*, **1991**, 113, (2), 686-687.
34. Hayden FG, Vote KM, Gordon Jr DR, Plaque inhibition assay for drug susceptibility testing of influenza viruses. *Antimicrob Agents Chemother*, **1980**, 17,865–870.
35. "*Orthomyxoviridae*: The Viruses and Their Replication." Fields Virology. 4th Ed (Illustrated). Lamb RA and Krug RM Ed. **2001**.
36. Gubareva LV, Robinson MJ, Bethell RC, Webster RG, Catalytic and framework mutations in the neuraminidase active site of influenza viruses that are resistant to 4-guanidino- Neu5Ac2en. *J Virol*, **1997**, 71, 3385–3390.
37. Herlocher ML, Truscon R, Elias S, Yen H-L, Roberts NA, Ohmit SE, Monto AS, Influenza viruses resistant to the antiviral drug oseltamivir: Transmission studies in ferrets. *J Infect Dis*, **2004**, 190, 1627–1630.
38. Yamashita M, Tomozawa T, Kakuta M, Tokumitsu A, Nasu H, Kubo S, CS-8959, a prodrug of the new neuraminidase inhibitor R-125489, shows long-acting anti influenza virus activity. *Antimicrob Agents Chemother*, **2009**, 53, (1), 186-192.
39. Mishin VP, Hayden FG, Gubareva LV, Susceptibilities of antiviral-resistant influenza viruses to novel neuraminidase inhibitors. *Antimicrob Agents Chemother*, **2005**, 49, 4515–4520.
40. Colman PM, Influenza virus neuraminidase: structure, antibodies, and inhibitors. *Protein Sci*, **1994**, 3, 1687-1696.
41. Krishnamurthy VM, Estroff LA, Whitesides GM, Multivalency in ligand design. In Methods and principles in medicinal chemistry; Jahnke W, Erlanson DA, Eds. Weinheim, Germany: Wiley-VCH. **2006**, (34), 11-53.
42. Kitov PI, Shimizu H, Homans SW, Bundle DR, Optimization of tether length in nonglycosidically linked bivalent ligands that target sites 2 and 1 of a shiga-like toxin. *J Am Chem Soc*, **2003**, 125, 3284–3294.
43. Lee CM, Weight AK, Haldar J, Wang L, Klibanov AM, Chen J, Polymer-attached zanamivir inhibits synergistically both early and late steps of influenza virus infection. *Proc Natl Acad Sci USA*, **2012**, 109, 20385-20390.
44. Andrews DM, Cherry PC, Humber DC, Jones PS, Keeling SP, Martin PF, Shaw CD, Swanson S, Synthesis and influenza sialidase inhibitory activity of analogues of 4- guanidino-Neu5Ac2en (zanamivir) modified in the glycerol side-chain. *Eur J Med Chem*, **1999**, 34, 563–574.

45. Chandler M, Bamford MJ, Conroy R, Lamont B, Patel B, Patel VK, Steeples IP, Storer R, Weir NG, Wright M, Williamson C, Synthesis of the potent influenza neuraminidase inhibitor 4-guanidino-Neu5Ac2en. X-ray molecular structure of 5-acetamido-4-amino-2,6-anhydro-3,4,5-trideoxy-D-*erythro*-L-guco-nononic acid. *J Chem Soc Perkin Trans*, **1995**, 1, 1173-1180.
46. Baumberger F, Vasella A, Schauer R, 4-Methylumbelliferyl 5-acetamido-3,4,5-trideoxy-α-D-*manno*-2-nonulopyranosidonic acid: synthesis and resistance to bacterial sialidases. *Helv Chim Acta*, **1986**, 69, 1927-1935.
47. Warner TG, Laura L, An azidoaryl thioglycoside of sialic acid. A potential photoaffinity probe of sialidases and sialic acid-binding proteins. *Carb Res*, **1998**, 176, (2), 211-218
48. Byramova NE, Mochalova LV, Belyanchikov IM, Matrosovich MN, Bovin NV, Synthesis of sialic acid pseudopolysaccharides by coupling of spacer-connected Neu5Ac with activated polymer. *J Carb Chem*, **1991**, 4, (10), 691-700
49. Ruiz MCdR, Amer H, Stanetty C, Beseda I, Czollner L, Shah P, Jordis U, Jueenburg B, Claben-Houben D, Hofinger A, Kosma P, Efficient synthesis of glycyrrhetinic acid glycoside/glucuronide derivatives using silver zeolite as promoter. *Carb Res*, **2009**, 344, 1063-1071.
50. Thomas RL, Sarkar AK, Kohata K, Abbas SA, Matta KL, Silver zeolite – effective catalyst for the regio-stereoselective formation of the Neu5Acα2-6 glycosyl linkage – synthesis of several sialosaccharides. *Tet Lett*, **1990**, 31, (20), 2825-2828.
51. McAuliffe JC, Rabuka D, Hindsgaul O, Synthesis of *O*-glycolyl-Linked Neuraminic Acids thorugh a Spirocyclic Intermediate. *Org Lett*, **2002**, 4, (18), 3067-3069.
52. Garegg PJ, Ossowski P, Silver zeolite as promoter in glycoside synthesis. The synthesis of β-D-Mannopyranosides. *Acta Chem Scan*, **1983**, 37B, (3), 249-250. P.J.
53. Haldar J, Weight AK, Klibanov AM, Preparation, application and testing of permanent antibacterial and antiviral coatings. *Nat Prot*, **2007**, 2, (10), 2412-2417.
54. Wetherall NT, Trivedi T, Zeller J, Hodges-Savola C, McKimm- Breschkin JL, Zambon M, Hayden FG, Evaluation of neuraminidase enzyme assays using different substrates to measure susceptibility of influenza virus clinical isolates to neuraminidase inhibitors. *J Clin Microbiol*, v41, 742–750.
55. Kati WM, Montgomery D, Maring C, Stoll VS, Giranda V, Chen X, Graeme LaverW, KohlbrennerW, Norbeck DW, Novel alpha and beta amino acid inhibitors of influenza virus neuraminidase. *Antimicrob Agents Chemother*, **2001**, 45, 2563–2570.

Chapter 3: Polymer-attached zanamivir is both an effective prophylactic and therapeutic *in vivo*

Most of the work presented in this chapter will be published in the following manuscript:

Weight AK, Belser JA, Tumpey TM, Chen J, Klibanov AM, Zanamivir conjugate to poly-*L*-glutamine is much more active against influenza viruses in mice and ferrets than the drug itself. **2013**, *J Pharm Sci*. Submitted.

Dr. Jessica Belser performed work with ferrets.

A. Introduction

Influenza is a persistent and constantly evolving threat to global human health. Despite annual vaccinations, hundreds of millions of people are infected and hundreds of thousands die from the infection each year[1,2]. The utility of currently approved antivirals, including the NA inhibitors Tamiflu™ (oseltamivir) and Relenza™ (zanamivir; ZA), continues to diminish as they are rendered ineffective by viral mutations[3,4]. Although the search for new small-molecule inhibitors is ongoing[5-8], identifying compounds with high potency both *in vitro* and *in vivo* has been only minimally successful.

In addition to enhanced binding seen in soluble protein or whole-virus studies of SA-containing polymeric inhibitors of hemagglutinin (HA)[9-13], some sialoligosaccharide-polyacrylate conjugates have also shown efficacy *in vivo* in mice[14,15]. Analysis of disease symptoms, lung histology, and mortality showed benefits of the polymeric species compared to untreated mice[14,15]. Interestingly, quantification of viral load was not directly assayed in any study. While promising, these studies were performed with polymers that, depending on uptake and metabolism, are potentially toxic and immunogenic[16-18]. Similarly, a ZA-containing polymer has only been assessed for its impact on survival[19]. All of these studies, however, failed to investigate un-adapted human influenza strains, a necessary corollary to *in vitro* studies with such viruses. Here, we examine viral loads in 1) infected mice and 2) human influenza-infected ferrets after treatment with biocompatible ZA-derivatized poly-*L*-glutamine inhibitor **12b**. Further, we assess the immunogenicity of conjugate **12b** in mice.

B. Results and Discussion

Polymeric inhibitor 12b is an effective prophylactic and therapeutic drug in the mouse and ferret models of infection

As described in Chapter 2, we have identified conjugate **12b** - poly-*L*-glutamine containing 10 mole percent of 7-*O*-alkyl-carbamate ZA analog **11** (Fig 3-1) - as a drug candidate that fills two unmet needs: it (i) is a potent inhibitor of drug-resistant strains of influenza viruses (Chapter 2) and (ii) has two modes of action inhibiting both neuraminidase activity and virus-endosome fusion[20]. Overall, conjugate **12b** with its long neutral backbone and short flexible linker was the most potent inhibitor of the derivatives examined (see Chapter 2). Herein, we have examined *in vivo* polymer-attached ZA **12b** (Fig 2-2) in the mouse and ferret models of influenza infection.

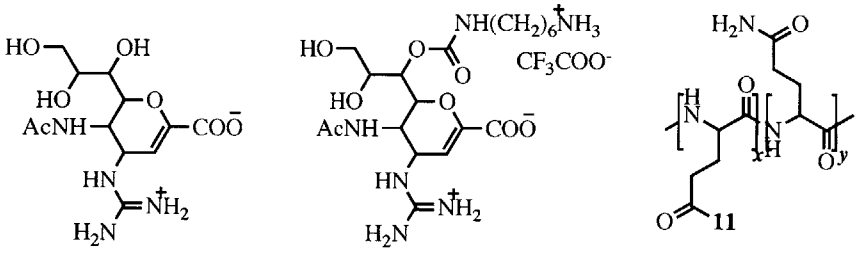

Figure 3-1. Chemical structures of ZA (**5**), ZA analog **11**, and poly-*L*-glutamine-attached **11** (polymeric **12b**).

First, we selected to study three virus strains known to replicate in animals: WSN and A/PR/8/34 (PR8) strains in mice and A/Nanchang/933/95 (Nanchang) in ferrets. We determined that Nanchang was an appropriate model strains because its growth was inhibited in the plaque assay by ZA and **12b** to a similar extent as other strains within the same subtype.

We then tested **12b** in a mouse model of influenza virus infection against WSN and PR8 strains. Briefly, mice were given intranasal doses of polymeric **12b**, ZA, or PBS (as a control),

immediately followed by intranasal infection. At 6, 24, and 48 h post-infection (p.i.), the mice were again given **12b**, ZA, or PBS intranasally (Fig 3-2A). Viral load was subsequently measured in whole-lung homogenates at 72 h p.i. Inhibitor doses were selected to be the lowest effective dose of ZA (determined by dose response studies with WSN and PR8 strains) and the equivalent molar dose of **12b** (in terms of ZA).

We determined viral titers from lung homogenates of WSN-infected mice using the plaque assay. Untreated mice had high titers of 10^7 pfu/mL (Fig 3-2B). When treated with ZA, the titers dropped 20-fold. Upon treatment with a molar equivalency of polymeric conjugate **12b**, the titers plummeted 190-fold, whereas no decrease was detected from treatment with poly-*L*-glutamine (**12**) alone. Thus **12b** is some 10-fold more potent than ZA at inhibiting WSN infection in mice.

For mice infected with PR8, we analyzed lung homogenates using qRT-PCR. Here, treatment with **12b** reduced viral load 11-fold more than that with ZA (Fig 3-2C), which correlates well with the above-referenced WSN study. Across both influenza strains and both analytical methods, therefore, we observed the same trend: polymeric conjugate **12b** was an order of magnitude more potent than ZA.

In mice, intranasal delivery of fluids post-infection with influenza virus – as we did in this study – has been shown to exacerbate the disease[21]. This fact can render experimental compounds less potent because they must inhibit significantly higher viral titers than presumed[21]. Consequently, our data may even underestimate the potency of polymeric inhibitor **12b** in the mouse model.

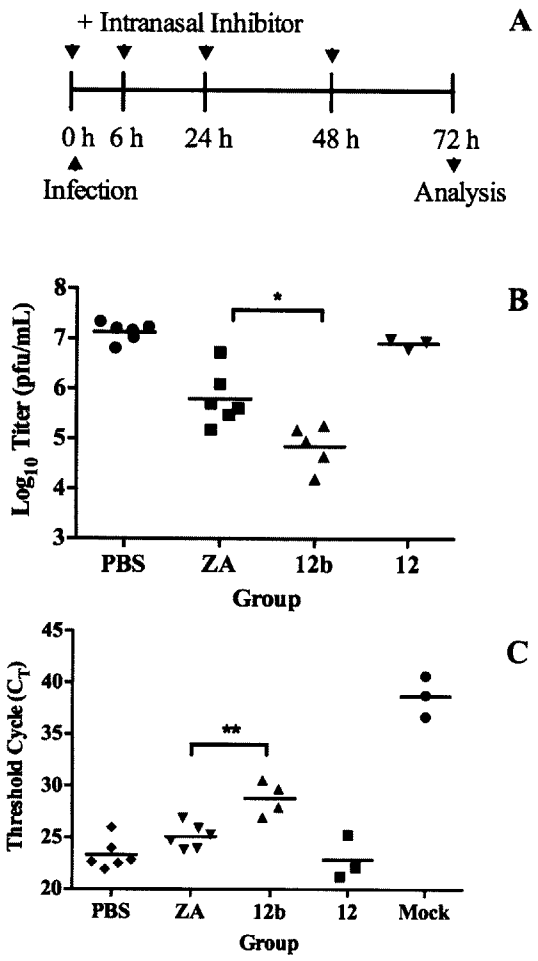

Figure 3-2. (**A**) Experimental design to determine the efficacy of ZA and **12b** in mice. (**B**) Viral titers (pfu/mL) from plaque assay of lung homogenates from mice infected with the WSN strain. Equimolar doses of ZA and **12b** were used; a 40-fold higher dose of backbone **12** was included as a control. The PBS group was infected and given vehicle only. Mice were dosed intranasally, immediately infected intranasally, and dosed again at 6, 24, and 48 h p.i.; their lungs were harvested 72 h p.i. Mock-infected group, not shown here due to scale, exhibited no plaques. (**C**) Viral load in lung homogenates of mice infected with PR8 strain. C_T values (higher numbers reflect lower relative levels of viral RNA expression) from qRT-PCR of lung homogenates. The mock group was given only vehicle. Experimental design was the same as in part (**B**). * $p < 0.05$ and ** $p < 0.01$ were determined by two-tailed Student's *t*-test. All reported values are the mean of at least three independent measurements.

Next, we determined the efficacy of **12b** in ferrets because this animal model of influenza infection is known to accurately reflect virus infectivity and antiviral activities in humans[22,23] . Ferret and humans share similar lung physiology and distribution of viral receptors[22,23]. On day 0, ferrets were infected with Nanchang virus, a clinically relevant human influenza strain. Beginning one day p.i., the ferrets were dosed daily with **12b**, ZA, or PBS (as a control) (Fig 3-3A). A nasal wash was collected from each ferret on days 2, 4, 6, and 8 to measure viral titer. On day 2 p.i., the ferrets given equimolar doses of ZA or **12b** (in terms of ZA) exhibited similar reductions in titer of 38- and 30-fold, respectively, compared to the PBS-treated group (Fig 3-3B). Treatment with **12b** continued to reduce viral titers significantly compared to PBS controls

- 30- and 20-fold on days 4 and 6 p.i., respectively, - whereas treatment with ZA did not (Fig 3-3B). Thus, polymeric conjugate **12b** is a more effective therapeutic agent than ZA in this highly relevant ferret model of influenza infection.

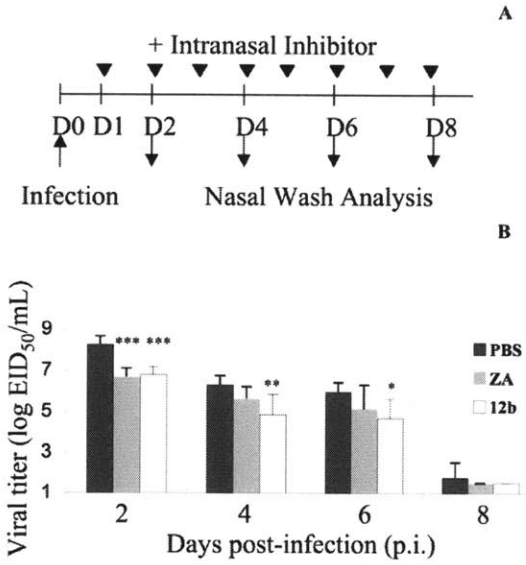

Figure 3-3. (**A**) Experimental design to determine therapeutic efficacy of **12b** in ferrets. (**B**) Viral titers in nasal washings of ferrets infected with Nanchang strain of influenza virus. Groups were treated with vehicle (PBS; black bars; n=6), or equimolar doses of ZA (grey bars, n=6) or **12b** (white bars, n=6). Statistically significant differences between PBS control and treated groups are represented by * $p < 0.05$ and ** $p < 0.01$ as determined by two-tailed Student's *t*-test. Mean values ± SEM represent triplicate measurements.

Polymeric inhibitor 12b **does not stimulate an immune response in mice**

Finally, we examined whether repeated dosing with **12b** stimulates an immune response, which could render **12b** ineffective. Although small molecules, such as ZA, do not typically elicit an antibody response, as part of a polymeric conjugate they can behave as haptens and become immunogenic[24-26]. To assess this possibility, we challenged mice intranasally for four days with a daily dose of PBS (as a control) or 40 μg of **12b**. This dose was 1) 40 fold higher than that used to inhibit virus infection in mice and 2) a dose similar to that used for modeling reactive airway disease and thus presumably high enough to stimulate inflammatory and immune responses in the lung[27]. Ten days after the first administration serum samples were collected. To increase the probability of antibody induction, after four weeks the mice were re-challenged for

three days with PBS or 40 μg of **12b** daily, and sera were again collected ten days later. Using **11**, **12**, and **12b** as capture antigens in an ELISA assay, we tested for the presence of specific IgG, IgM, and IgA in the serum samples. Only a background level of immunoglobulin was detected in the mice given **4b** before, after primary, and after secondary challenge, the same as in control mice given PBS (Table 3-1).

Table 3-1. Drug-specific serum immunoglobulin ELISA titers from mice treated with high-dose **12b** or PBS (as a control) were measured pre-challenge ("Pre-"), 10 days after primary challenge ("Primary"), and 10 days after secondary challenge ("Secondary").

Capture antigen	Time point (relative to challenges)	Reciprocal specific antibody titers[a]					
		IgG		IgM		IgA	
		PBS	**12b**	PBS	**12b**	PBS	**12b**
ZA	Pre-	<20	<20	<20	<20	<20	<20
	Primary	<20	<20	<20	<20	<20	<20
	Secondary	<20	<20	20	20	<20	<20
12	Pre-	<20	<20	20	20	20	20
	Primary	<20	<20	20	20	20	20
	Secondary	<20	<20	20	20	20	20
12b	Pre-	<20	<20	<20	<20	<20	<20
	Primary	<20	<20	20	<20	20	<20
	Secondary	<20	<20	20	20	20	20
12j	Pre-	<20	<20	40	40	20	20
	Primary	<20	<20	40	20	20	20
	Secondary	<20	<20	40	40	20	20

[a] The titers are reported as the reciprocal of the least dilute sample with signal 2-fold above background and are the average of at least two measurements of each sample within each group (n=3). Serum dilutions were 1:20, 1:40, and 1:100.

Sometimes, however, the more hapten that is present in the capture antigen, the more sensitive the ELISA to hapten- or conjugate-specific antibodies[24,28,29]. Even when **12j** – with 20 mole-percent **11** (Fig 3-1) – was used as a capture antigen, again only background levels of immunoglobulin were detected in **12b**-treated mice, as in PBS-treated mice (Table 3-1). Thus,

upon repeated challenge with a dose 40-fold higher than that used in the aforementioned infection studies, no neutralizing antibodies against **12b** or any of its components were detected.

Conclusion

In summary, we have demonstrated herein that optimized polymeric drug species **12b** is an efficacious inhibitor of influenza infections in the respiratory tracts, reducing viral titers up to 190-fold *in vivo* and without stimulating an immune response. These results, coupled with other beneficial properties of **12b** – namely, multiple modes of inhibition[20] and efficacy against drug-resistant virus strains (Chapter 2) – make it a promising inhibitor of influenza infection for further development.

Acknowledgements

I am thankful for Camille Jusino, Amanda Souza, and Ryan Phennicie who patiently taught me about and assisted with mouse husbandry and handling throughout these studies. I gratefully acknowledge Dr. Adam Drake and Dr. Bettina Iliopoulou for sharing their extensive knowledge about animal experiment design, tissue processing, and serum analysis. Also, I would like to thank Dr. Peter Bak for providing mouse serum for assay optimization and control studies, and Dr. Terrence Tumpey and Dr. Jessica Belser for performing ferret work.

C. Materials and Methods

Influenza viruses

Plaque-purified influenza A/WSN/33 (WSN; H1N1) was cultured in E4HG medium from MDCK cells (ATCC; Manassas, VA), clarified, and filtered through a 0.2-μm filter to remove aggregates. Influenza virus strains A/Wuhan/359/95 (Wuhan; H3N2), A/turkey/MN/833/80 (TKY; H4N2), and A/turkey/MN/833/80/E119D drug-resistant mutant (TKY E119D) were obtained from the Centers for Disease Control and Prevention (CDC) (Atlanta, GA) and propagated as previously described[30]. Sucrose-gradient purified influenza A/PR/8/34 (PR8; H1N1) was obtained from Charles River Laboratories in HEPES-saline buffer (Wilmington,

MA) and diluted with PBS (pH 7.2) before use. Viral titers were determined by serial titration in the 12-well format plaque assay[31]. Stocks of influenza A/Nanchang/933/95 (Nanchang) H3N2 virus were grown in the allantoic cavities of 10-day-old embryonated hens' eggs at 34°C for 48-72 h. Pooled allantoic fluid was clarified by centrifugation and stored at -70°C. Fifty percent egg infectious dose (EID_{50}) titers were determined by serial titration of virus in eggs and calculated by the method of Reed and Muench[32].

Ethics statement

All mouse procedures were approved by the MIT Committee on Animal Care under protocol #0310-027-13. Animal studies were performed in accordance with the IACUC guidelines at the CDC under protocol #2195TUMFERC-A3: "Studies on the Pathogenesis and Transmission of Recombinant Influenza Viruses in Ferrets".

Mouse experiments

Male Balb/C mice at 8 weeks (Jackson Laboratories, Bar Harbor, ME) were used in this study. They were anesthetized with intraperitoneal avertin injection and dosed intranasally in one nostril with a 25 μL solution of either PBS (vehicle control), ZA, **12**, or **12b**. Within 10 min, mice were then infected with 25 μL of virus solution in PBS (1,000 pfu/mouse) delivered in the same nostril. At 6, 24, and 48 h post-infection (p.i.), mice were again given PBS, ZA, **12**, or **12b**.

Inhibitor doses were 0.028 μmol/kg for ZA, an equimolar dose of **12b** (0.028 μmol/kg on a ZA basis; 0.24 μmol/kg on a monomer basis), and 11 μmol/kg **5** (40-fold molar equivalency on a monomer basis). Group sizes were: PBS – 6 mice, **12** – 3 mice, **12b** – 4 mice, and mock infection – 3 mice. For WSN-infection, 5 mice were given ZA. For PR8-infection, 6 mice were given ZA. Animals were euthanized with CO_2 at 72 h post-infection (p.i). Whole mouse lung

was harvested, rinsed in ice-cold homogenization buffer (50 mL of 1X PBS plus 150 μL of 35% BSA and 500 μL of a solution of 10,000 IU/ml penicillin G and 10,000 mg/mL streptomycin (JR Scientific, Woodland, CA)), flash-frozen on dry ice in 1 mL of ice-cold homogenization buffer, and stored at -80°C until processing.

For PR8-infected mice, lungs were homogenized using a Branson Sonifier 250 with a $^1/_8$" tapered tip probe (Branson Ultrasonics, Danbury, CT). Total RNA was extracted from 170 μL of clarified lung homogenate using the PureLink Viral RNA/DNA Kit (Invitrogen, Carlsbad, CA) according to manufacturer's instructions. Viral RNA was eluted in Tris-EDTA buffer (pH 8.0) and stored at -80°C. Quantification of viral RNA was performed using the RNA Ultrasense One-step qRT-PCR System (Invitrogen) according to manufacturer's instructions after treatment with RNase-free DNase (Ambion, Austin, TX). Primer and probe to detect the encoding region for the M1 matrix protein were used at concentrations of 1,900 nM and 754 nM, respectively, in a total reaction volume of 40 μL. Sequences of influenza A-specific primers and probe (IDT, Coralville, IA) were previously established[33]. A Roche LightCycler® instrument was used for real-time reverse-transcriptase PCR using the following program: 45°C for 30 min, 95°C for 2 min, and 50 cycles of 95°C for 5 sec, 55°C for 10 sec, and 72°C for 10 sec. All samples and a standard curve of serially diluted un-passaged virus were run on the same reaction plate. Levels of viral RNA in lung homogenates[34] are expressed as threshold cycle (C_T), determined using LightCycler® 480 System software v. 1.5. To confirm that any residual polymer in homogenates did not interfere with RNA extraction, a sample of stock virus and a sample of homogenate from an untreated mouse were spiked with **5** before extraction and PCR. A standard curve of the spiked virus and C_T value of the spiked homogenate were in agreement with that of the un-passaged virus. Thus, the observed C_T values reflect robust purification.

For WSN-infected mice, lungs were homogenized using a Dounce homogenizer on ice. Viral titers of WSN in clarified murine lung homogenates were determined by 12-well format plaque assay and expressed in pfu/mL[30,31,35]. To exclude the possibility that the reduced titers measured in treated groups were a result of residual ZA or **12b** in lung homogenates, one uninfected mouse was dosed with each inhibitor. Lung homogenates from these mice were mixed in equal volume with that of infected but untreated (PBS control) mice. No significant difference in virus titer was observed; the reduction in titer seen with treated mice does indeed reflect *in vivo* inhibition.

Immune response studies were performed with 8-week old male Balb/C mice. Mice were split into two groups of four, anesthetized with intraperitoneal avertin and challenged with 40 μL of PBS or 40 μL of 1 mg/mL **12b** at 0, 6, 24, and 48 h. After 4 weeks, mice were re-challenged with three administrations of 40 μL of PBS or 40 μL of 1 mg/mL **12b**. Serum samples were collected "pre-challenge" from a tail-vein 3 weeks before initial challenge. "Primary challenge" and "secondary challenge" samples were collected 10 days after initial challenge and secondary challenge. Serum samples were separated using BD Microtainer serum separator tubes (Becton Dickinson, Franklin Lakes, NJ) and stored at -80°C.

ELISA

ELISA to determine total and specific immunoglobulin levels in mouse serum was performed according to a modified literature procedure using Costar Universal Bind plates (Corning, Tewksbury, MA)[20]. Antibody pairs and standards (mouse IgG, IgM, and IgA) and TMB substrate were used directly from Ready-Set-Go Mouse Ig kits (eBioscience, San Diego, CA). For detection of **12b**-, **12**-, or ZA-specific antibodies by ELISA, 50 μL of 0.01 mg/mL **12b** or **12**, and 50 μL of 0.1 mg/mL **11** were incubated overnight at 4°C. Capture antibodies were

incubated according to manufacturer's instructions. For washing, 1% PBST (1% BSA (w/v) and 0.05% (v/v) Tween 20 in PBS) were used. Blocking (4 h, RT) and serum dilutions (100 μL total incubation volume) were performed with 2% PBST (2% BSA (w/v) and 0.05% (v/v) Tween 20 in PBS). After washing five times, HRP-conjugated antibody was incubated at RT for 3 h, and detection performed as per manufacturer's instruction. Serum from all experimental mice plus serum from an untreated but WSN-infected mouse (positive control collected at 2.5 weeks p.i.) were included on each plate. Sensitivity of the assay was 1.5 ng/mL for IgG, 0.7 ng/mL for IgM, and 0.7 ng/mL for IgA.

Ferret experiment

Adult male Fitch ferrets, five months of age (Triple F Farms, Sayre, PA), serologically negative by hemagglutination-inhibition assay for currently circulating influenza viruses, were used in this study. Six ferrets per group were anesthetized with an intramuscular injection of a ketamine hydrochloride (24 mg/kg)-xylazine (2 mg/kg)-atropine (0.05 mg/kg) cocktail and infected intranasally with Nanchang virus at 10^5 EID_{50} in a final volume of 1 mL of PBS. Ferrets were sedated by Ketamine before intranasal delivery of 500 μL (250 μL per nostril) of 6 μmol/kg bodyweight of **12b** in PBS; six control ferrets received vehicle (PBS) only. Ferrets receiving treatment with ZA were given 0.7 μmol/kg bodyweight in PBS administered intranasally. Ferrets received daily dosing of PBS, **12b**, or ZA over a period of eight days beginning 24 h p.i. Ferrets were monitored daily for changes in body weight and temperature, as well as clinical signs of illness. Body temperatures were measured using an implantable subcutaneous temperature transponder (BioMedic Data Systems, Seaford, DE). Virus shedding was measured in nasal washes collected on days 2, 4, 6, and 8 p.i. from anesthetized ferrets as previously described[36]. Virus titers in nasal washes were determined in eggs and expressed as EID_{50}/mL.

Statistical analysis

Unpaired two-tailed Student's *t*-test was performed using Prism 6 software.

D. References

1. Dushoff J, Plotkin JB, Viboud C, Earn DJD, Simonsen L, Mortality due to influenza in the United States—an annualized regression approach using multiple-cause mortality data. *Am J Epidemiol*, **2005**, 163, 181–187.
2. Graham-Rowe D, Racing against the flu. *Nature*, **2011**, 480, S2–S3.
3. Palmer R, Lines of defense. *Nature*, **2011**, 480, S9–S10.
4. Gubareva LV, Molecular mechanism of influenza virus resistance to neuraminidase inhibitors. *Virus Res*, **2004**, 103, 199–203.
5. Ortigoza MB, Dibben O, Maamary J, Martinez-Gil L, Leyva-Grado VH, Abreu P, Ayllon J, Palese P, Shaw ML, A novel small molecule inhibitor of influenza A viruses that targets polymerase function and indirectly induces interferon. *PLoS Pathog*, **2012**, 8, (4), e1002668.
6. Koyama K, Takahashi M, Oitate M, Nakai N, Takakusa H, Miura S, Okazaki O, CS-8958, a prodrug of the novel neuraminidase inhibitor R-125489, demonstrates a favorable long-retention profile in the mouse respiratory tract. *Antimicrob Agents Chemother*, **2009**, 53, 4845–4851.
7. An J, Lee DCW, Law AHY, Yang CLH, Poon LLM, Lau ASY, Jones SJM, A novel small-molecule inhibitor of the avian influenza H5N1 virus determined through computational screening against the neuraminidase. *J Med Chem*, **2009**, 52, 2667-2672.
8. Jablonski JJ, Basu D, Engel DA, Geysen HM, Design, synthesis, and evaluation of novel small molecule inhibitors of the influenza virus protein NS1. *Bioorg Med Chem*, **2012**, 20, 487-497.
9. Mammen M, Choi S-K, Whitesides GM, Polyvalent interactions in biological systems: Implications for design and use of multivalent ligands and inhibitors. *Angew Chem Int Ed*, **1998**, 37, 2754–2794.
10. Sigal GB, Mammen M, Dahmann G, Whitesides, Polyacrylamides bearing pendant α-sialoside groups strongly inhibit agglutination of erythrocytes by influenza virus: the strong inhibition reflects enhanced binding through cooperative polyvalent interactions. *J Am Chem Soc*, **1996**, 118,3789-3800.
11. Mammen M, Dahmann G, Whitesides GM, Effective inhibitors of hemagglutination by influenza virus synthesized from polymers having active ester groups. *J Med Chem*, **1995**, 38, 4179–4190.
12. Matrosovich MN, Mochalova LV, Marinina VP, Byramova NE, Bovin NV, Synthetic polymeric sialoside inhibitors of influenza virus receptor-binding activity. *FEBS Lett*, **1990**, 272, (1,2), 209-212.
13. Mochalova LV, Tuzikov AB, Marinina VP, Gambaryan AS, Byramova NE, Bovin NV,

Matrosovich MN, Synthetic polymeric inhibitors of influenza virus receptor-binding activity suppress virus replication. *Antiviral Res*, **1994**, 23, 179-190.

14. Gambaryan AS, Tuzikov AB, Chinarev AA, Juneja LR, Bovin NV, Matrosovich MN, Polymeric inhibitor of influenza virus attachment protects mice from experimental influenza infection. *Antiviral Res*, **2002**, 55, 201-205.
15. Gambaryan AS, Boravleva EY, Matrosovich TY, Matrosovich MN, Klenk H-D, Moiseeva EV, Tuzikov AB, Chinarev AA, Pazynina GV, Bovin NV, Polymer-bound 6' sialyl-*N*-acetyllactosamine protects mice infected by influenza virus. *Antiviral Res*, **2005**, 68, 116-123.
16. King DJ, Noss RR, Toxicity of polyacrylamide and acrylamide monomer. *Rev Environ Health*, **1989**, 8, 3-16.
17. Xi TF, Fan CX, Feng XM, Wan ZY, Wang CR, Chou LL, Cytotoxicity and altered c-myc gene expression by medical polyacrylamide hydrogel. *J. Biomed Mat Res*, **2006**, 78A, 283-290.
18. Totani K, Kubota T, Kuroda T, Muarata T, Hidari KI-P, Suzuki T, Suzuki Y, Kobayashi K, Ashida H, Yamamoto K, Usui T, Chemoenzymatic synthesis and application of glycopolymers containing multivalent sialyloligosaccharides with a poly(L-glutamic acid) backbone for inhibition of infection by influenza viruses. *Glycobiol*, **2003**, 13, 315-326.
19. Masuda T, Yoshida S, Arai M, Kaneko S, Yamashita M, Honda T, Synthesis and anti-influenza evaluation of polyvalent sialidase inhibitors bearing 4-guanidino-Neu5ac2en derivatives. *Chem Pharm Bull*, **2003**, 51, 1386-1398.
20. Lee CM, Weight AK, Haldar J, Wang L, Klibanov AM, Chen J, Polymer-attached zanamivir inhibits synergistically both early and late steps of influenza virus infection. *Proc Natl Acad Sci USA*, **2012**, 109, 20385-20390.
21. Smee DF, von Itzstein M, Bhatt B, Tarbet EB, Exacerbation of influenza virus infections in mice by intranasal treatments and implications for evaluation of antiviral drugs. *Antimicrob Agents Chemother*, **2012**, 56, 6328-6333.
22. Bouvier NM, Lowen AC, Animal models for influenza virus pathogenesis and transmission. *Viruses*, **2010**, 2, 1530-1563.
23. Belser JA, Katz JM, Tumpey TM, The ferret as a model organism to study influenza A virus infection. *Disease Models Mechanisms*, **2011**, 4, 575-579.
24. Lemus R, Karol MH, Conjugation of haptens. *In* Jones ME, Lympany P, Eds. Methods in Molecular Medicine, **2008**, Vol. 138: Allergy Methods and Protocols. Totowa, NJ: Humana Press, pp. 167-182.
25. Sylvia LM, Drug allergy, pseudoallergy, and cutaneous diseases. *In* Tisdale JE, Miller DA, Eds. Drug-Induced Diseases, Prevention, Detection, and Management, **2010**, Bethesda, MD: American Society of Health-System Pharmacists, pp. 57-61.
26. Mansour NA, Alassuity AS, Immunoassays for the detection of pesticides. *In* Valdes JJ, Sekowski JW, Eds. Toxicogenomics and Proteomics, **2004**, Vol. 356: NATO Science Series, I:Life and Behavioural Sciences, Lansdale PA: IOS Press, pp. 159-180.

27. Reuter S, Dehzad N, Martin H, Bohm L, Becker M, Buhl R, Stassen M, Taube C. TLR3 but Not TLR7/8 Ligand Induces Allergic Sensitization to Inhaled Allergen. *J Immunol*, **2012**, 188, (10), 5123-5131.
28. Pedersen MK, Sorensen NS, Heegaard P, Beyer NH, Bruun L, Effect of different hapten-carrier conjugation ratios and molecular orientations on antibody affinity against a peptide antigen. *J Immunol Methods*, **2006**, 311, (1-2), 198-206.
29. Hu K, Huang X, Jiang Y, Qiu J, Fang W, Yang X, Influence of hapten density on immunogenicity for anti-ciprofloxacin antibody production in mice. *BioScience Trends*, **2012**, 6, (2), 52-56.
30. Haldar J, de Cienfuegos LA, Tumpey TM, Gubareva LV, Chen J, Klibanov AM, Bifunctional polymeric inhibitors of human influenza A viruses. *Pharm Res*, **2010**, 27, 259-263.
31. Haldar J, Weight AK, Klibanov AM, Preparation, application and testing of permanent antibacterial and antiviral coatings. *Nat Prot*, **2007**, 2, (10), 2412-2417.
32. Reed LJ, Muench H, A simple method of estimating fifty percent endpoints. *Am J Hygiene*, **1938**, 27, 493-497.
33. van Elden LJR, Nijhuis M, Schipper P, Schuurman R, van Loon AM, Simultaneous detection of influenza viruses A and B using real-time quantitative PCR. *J Clin Microbiol*, **2001**, 39, 196–200.
34. Smith JS, Tian J, Lozier JN, Byrnes AP, Severe pulmonary pathology after intravenous administration of adenovirus vectors in cirrhotic rats. *Molec Ther*, **2004**, 9, 932-941.
35. Zhang L, Hartshorn KL, Crouch EC, Ikegami M, Whitsett JA, Complementation of pulmonary abnormalities in SP-D(-/-) mice with an SP-D/conglutinin fusion protein. *J Biol Chem*, **2002**, 277, 22453-22459.
36. Zitzow LA, Rowe T, Morken T, Shieh WJ, Zaki S, Katz JM, Pathogenesis of avian influenza A (H5N1) viruses in ferrets. *J Virol*, **2002**, 76, 4420-4429.

Chapter 4: Reducing the viscosity of highly concentrated antibody formulations

Most of the work presented in this chapter will be published in the following manuscript:

Srinivasan C, Weight AK, Bussemer T, Klibanov AM, Non-aqueous suspensions of antibodies are much less viscous than equally concentrated aqueous solutions. **2013**, *Pharm Res.* Accepted.

Dr. Charu Srinivasan performed work with PEG- and salt-induced γ-globulin suspensions and collaborated on work with γ-globulin suspensions in aqueous and non-aqueous organic solvents.

A. Introduction

Monoclonal antibody (MAb) therapeutics are increasingly common in clinical practice[1-3], generally demonstrating high specificity and selectivity and low toxicity when humanized or fully human[4,5]. They are frequently used to treat cancer, autoimmune disease, infectious disease, allergic inflammations (such as asthma), and to prevent post-transplantation rejection[6,7]. Due to low bioavailability – a result of high molecular weight, polarity, and rapid degradation in the stomach[7,8] – no MAbs are currently administered orally. Instead, MAbs are delivered through parenteral routes – typically intravenous infusion – that can require travel to a medical practitioner[7,9]. Though estimated to account for approximately 20% of the pharmaceutical pipeline[10], a major impediment to increased utility, practicality, and patient compliance with MAb therapies is the need for highly concentrated formulations that would permit subcutaneous injection in a patient's home.

MAbs tend to have a long elimination half-life on the order of days[7], though sufficient therapeutic potencies of chimeric or humanized MAbs often require protein doses of hundreds of milligrams due to low specific activties[10,11]. The U.S. Food and Drug Administration (FDA), however, does not permit subcutaneous injections of volumes over ~1.5 mL with a viscosity exceeding ~50 centipoise (cP)[11]. Such a requirement is often difficult to meet since multi-hundred-mg/mL protein solutions are typically very viscous. This thick consistency with a strong resistance to flow makes concentrated protein formulations challenging to handle and administer to patients. Hence lowering their viscosity is critical to harness the benefits of protein-based pharmaceuticals.

Recently, new strategies toward the aforementioned goal, such as the addition of hydrophobic salts[12,13] or of molecular crowding agents[14,15] to concentrated protein solutions,

have afforded much reduced viscosities. An alternative promising approach is to replace aqueous protein solutions with crystalline suspensions[10,16]. However, crystallizing antibodies is unpredictable and time-consuming due to their high molecular weight, abundant glycosylation, and structural flexibility[3,10]. We overcome this drawback, and in this chapter demonstrate that viscosities of suspensions in neat ethanol and numerous other organic solvents, made from an amorphous powder of γ-globulin (a model protein for monoclonal antibodies) or monoclonal antibodies, are drastically lower than those of equally concentrated aqueous solutions.

B. Results and discussion

PEG nanosuspensions of γ-globulin are more viscous than the corresponding solution

Typically, highly concentrated solutions of therapeutic proteins are very viscous making injections difficult. Herein we have explored this phenomenon and methods of circumventing it by employing concentrated suspensions of amorphous protein powders, rather than conventional aqueous solutions. Bovine γ-globulin has been used as a model antibody in this study.

First, we investigated concentration dependence of the viscosity of aqueous solutions of γ-globulin. As seen in Fig 4-1, we observed the expected[13,17,18] exponential (as opposed to linear) rise in solution viscosity as protein concentration increased. At 300 mg/mL, for example, the γ-globulin solution viscosity at 25°C is 370 ± 20 cP, far higher than that permitted for subcutaneous injections[12]. Using dynamic light scattering, we determined that the average effective diameter of γ-globulin molecules in this solution is 37 nm (Table 4-1). Protein molecules in this solution must be in close proximity to each other, with an average intermolecular distance of less than one third of a molecular diameter (based on a spherical-shape approximation with a Stokes diameter of 10.5 nm for γ-globulin[19]). The resultant intimate intermolecular contacts and abundant hydrophobic and electrostatic interactions[13] create a strong

resistance to flow, or high viscosity. This high γ-globulin concentration of 300 mg/mL was selected for most of the subsequent study.

We next investigated PEG4000 – typically used in relatively low concentrations as a macromolecular crowder[10,14,15,20] – as a precipitating agent. Addition of 1% PEG4000 to a 300 mg/mL γ-globulin solution produced a translucent mixture suggesting a nanosuspension (i.e., having a particle diameter comparable with a half of the wavelength of visible light). Indeed, particle size analysis thereof by dynamic light scattering yielded a diameter of 110 nm (Table 4-1). Henceforth, translucency was used as a tentative visual indicator of nanosuspension formation.

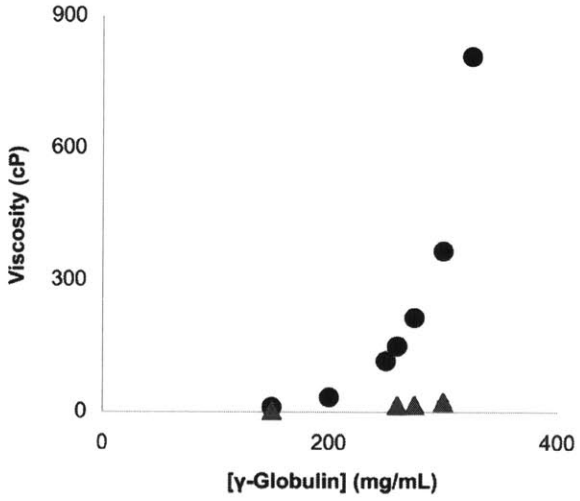

Figure 4-1. Concentration dependence of viscosities of solutions (circles) and suspensions (triangles) of γ-globulin at 25°C. Solutions were prepared in de-ionized water to give a final pH of 6.0 and suspensions using neat ethanol. The data points incorporate the standard deviations which, however, are smaller than the symbols.

The viscosity of this PEG-induced nanosuspension was 530 cP, or 1.4-fold greater than that of a γ-globulin solution of the same concentration (Table 4-1). We determined that this increase in viscosity was not due to irreversible denaturation or aggregation of the protein upon precipitation with PEG; when the nanosuspension was diluted, thereby re-dissolving the protein,

the average particle diameter dropped to 36 nm, i.e., the same as for γ-globulin in the original solution (Table 4-1).

Table 4-1. Viscosities at 25°C and protein particle sizes of 300 mg/mL γ-globulin formulations in 20 mM histidine-HCl buffer (final pH 5.2).

Formulation	Viscosity (cP)	Particle diameter (nm)
Solution	370 ± 17	37 ± 6.1
Suspension formed by (1% w/v PEG4000)	530 ± 12	110 ± 2.3
Dissolved suspension	n.d.	36 ± 1.7

Excipients reduce viscosity comparably in both γ-globulin nanosuspensions and solutions

We previously ascertained that hydrophobic intermolecular interactions are largely responsible for high viscosities of concentrated solutions of monoclonal antibodies[13]. To test this possibility for γ-globulin, we added cationic, anionic, non-ionic, or zwitter-ionic surfactants to its PEG-induced nanosuspension to disrupt hydrophobic contacts. All tested surfactants slightly lowered the viscosities of PEG nanosuspensions of γ-globulin, with the most potent (non-ionic Pluronic F68) affording a 30% drop (Table 4-2). A comparable viscosity-lowering effect, however, was also observed for γ-globulin solutions. Though marginal in magnitude and certainly falling short of our ultimate objective, these effects suggest that hydrophobic interactions do play a role in the high viscosities of concentrated solutions and nanosuspensions of γ-globulin.

To test whether another factor – electrostatic interactions – contributes to viscosity increases in nanosuspensions, we added 1 M salts to weaken these ionic interactions. Both increasing and decreasing viscosities were observed in PEG-induced nanosuspensions of γ-globulin depending on the salt (Table 4-3). Surprisingly, the addition of NaCl, recently reported to greatly decrease the viscosity of monoclonal antibody solutions[17], raised the viscosity of the

suspension some 2.5 fold. The effects of salt excipients on solution viscosity thus seem to be both protein-dependent and not applicable to suspensions.

Table 4-2. Viscosities at 25°C of 300 mg/mL γ-globulin solutions and 1% (w/v) PEG-induced nanosuspensions in the presence of surfactants in 20 mM aqueous histidine-HCl buffer (final pH of 5.2)

Surfactant		Viscosity (cP)[a]	
Classification	Compound (%w/v)	Solution	Nanosuspension
None		370 ± 17	530 ± 12
Cationic	BKC[b] (0.15)	300 ± 6.8	400 ± 3.2
	BKC (0.04)	310 ± 3.6	390 ± 2.0
Anionic	SDS[c] (0.1)	320 ± 1.7	400 ± 2.4
Non-ionic	Tween 80 (0.1)	340 ± 3.4	480 ± 3.1
	Tween 80 (0.001)	340 ± 17	470 ± 7.6
	Pluronic F68 (0.06)	240 ± 1.0	400 ± 4.9
	Pluronic F68 (0.01)	n.d.	380 ± 12
Zwitterionic	CHAPS[d] (1.2)	320 ± 3.8	410 ± 6.1
	CHAPS (0.3)	n.d.	440 ± 11

n.d. = not determined

[a] The surfactants themselves, even at the highest concentrations used, made negligible contributions to observed viscosities. The *p*-values reflecting the viscosity differences between solutions and the corresponding nanosuspensions were in all cases no greater than 0.01. The same applies to the viscosity differences between the nanosuspension without surfactant and those with surfactants, except that in this case no *p*-value exceeded 0.03.

[b] Benzalkonium chloride

[c] Sodium dodecyl sulfate

[d] 3-[(3-Cholamidopropyl)dimethylammonio]-1-propanesulfonate

Among the other salts, addition of arginine-HCl (a common pharmaceutical additive[8]) showed the most potent viscosity reducing effect, decreasing the viscosity of a 300 mg/mL γ-globulin nanosuspension 6-fold (Table 4-3). As seen in the table, ethanolamine-HCl and Tris-HCl were also quite potent, reducing viscosity 3.8- and 4.1-fold, respectively. Although these hydrochlorides substantially decreased γ-globulin nanosuspension viscosities, their effect on a 300 mg/mL protein solution was equally beneficial (Table 4-3), thus making formation of nanosuspensions superfluous.

Table 4-3. Viscosities at 25°C of 300 mg/mL γ-globulin solutions and 1% (w/v) PEG-induced nanosuspensions in the presence of various 1 M salts in 20 mM aqueous histidine-HCl buffer (final pH of 5.2).

Salt	Viscosity (cP)	
	Nanosuspension	Solution
None	530 ± 12	366 ± 17
Arginine-HCl	89 ± 1.6	89 ± 0.30
Tris-HCl	130 ± 2.1	110 ± 5.3
$NH_2(CH_2)_2OH$ HCl	140 ± 4.5	150 ± 17
Guanidine-HCl	280 ± 3.1	n.d.
NH_4Cl	390 ± 35	n.d.
$NaNO_3$	540 ± 6.0	n.d.
KCl	770 ± 24	n.d.
L-Lysine-HCl	780 ± 32	n.d.
D-Lysine-HCl	880 ± 23	n.d.
NaCl	1300 ± 60	n.d.
CH_3COONa	1500 ± 230	n.d.

n.d. not determined

Table 4-4. Viscosities at 25°C of 300 mg/mL γ-globulin solutions and 1% (w/v) PEG-induced nanosuspensions in the presence of various 1 M arginine salts in 20 mM histidine-HCl buffer (final pH of 5.2).

Anion	Viscosity (cP)	
	Nanosuspension	Solution
None	530 ± 12	366 ± 17
CH_3COO^-	80 ± 9.5	121 ± 13
Cl^-	89 ± 1.6	89 ± 0.30
NO_3^-	89 ± 4.2	94 ± 3.2
Succinate	100 ± 2.6	130 ± 4.3
Fumarate	105 ± 5.2	100 ± 4.9
$HCOO^-$	110 ± 11	n.d.
CF_3COO^-	110 ± 7.9	n.d.
Camphorsulfonate	140 ± 1.0	n.d.
$CH_3CH_2COO^-$	150 ± 11	n.d.
SO_4^{2-}	160 ± 0.13	n.d.
Citrate	180 ± 3.7	n.d.
Glutamate	210 ± 17	n.d.

n.d. not determined

We then investigated effects on viscosity due to the nature of the anion in arginine salts. As seen in Table 4-4, analog arginine acetate was the most effective, reducing nanosuspension viscosity 6.6-fold. In fact, it is one of only two salts affording PEG-induced γ-globulin nanosuspensions that are less viscous than the corresponding solution (Table 4-4). Overall, however, we continue to observe the same general trend: even when modification of PEG-induced aqueous nanosuspensions with surfactants or salts lowered viscosity, the effect was comparable to that achieved by adding the same excipients to a protein solution.

We therefore explored still additional precipitating agents. 0.43 M sodium citrate[20] formed a translucent nanosuspension of γ-globulin with a viscosity of 770 cP and an average particle diameter of 120 nm (Table 4-5). However, this viscosity was higher than that of the corresponding solution. In aqueous ethanol, a common system for precipitating proteins[21,22], a

translucent nanosuspension with particle diameter of 100 ± 9.9 nm formed in a 50% (v/v) solution. Curiously, however, ethanol-induced nanosuspensions formed only at low protein concentrations such as 15 mg/mL, but had a 5-fold higher viscosity than the corresponding solution (Table 4-6). Thus, as with sodium citrate, a solution is again less viscous than a nanosuspension.

Table 4-5. Viscosities at 25°C and protein particle sizes of 300 mg/mL γ-globulin solutions and nanosuspensions (induced by 0.43 M Na citrate) in 20 mM aqueous histidine-HCl buffer (final pH of 5.2).

Formulation	Additive	Viscosity (cP)	Particle Diameter (nm)
Solution	None	370 ± 17	37 ± 6.1
Nanosuspension		770 ± 33	120 ± 3.7
Solution	1 M Arginine acetate	120 ± 13	n.d.
Nanosuspension		110 ± 3.7	n.d.

n.d. = not determined

Table 4-6. Viscosities at 25°C and protein particle sizes of a 15 mg/mL γ-globulin solution and ethanol-induced nanosuspension in 20 mM aqueous histidine-HCl buffer (final pH of 5.2).

Formulation	Viscosity (cP)	Particle Diameter (nm)
Solution	4.0 ± 0.14	21 ± 0.45
Nanosuspension	20 ± 0.10	110 ± 9.9

Ethanolic suspensions of γ-globulin are less viscous than solutions

Protein nanoparticles comprise a bimodal population: those protein molecules buried within the particle and those on the surface. Decreasing the fraction of exposed protein molecules should reduce viscosity. When formed with sodium citrate, PEG, or ethanol, nanoparticles have a mean diameter of 113 nm (Tables 4-1, 4-5, and 4-6). A straightforward calculation (for an idealized spherical nanoparticle with a diameter of 113 nm composed of idealized spherical protein particles with a diameter of 37 nm, all but one protein molecule will be on the surface: 113 nm - 2 x 37 nm = 39 nm; in other words, the nanoparticle contains

essentially three protein molecules across) reveals that the vast majority of the protein molecules in particles of this size are on the surface. Hence such nanoparticles fail to effectively shield a significant fraction of γ-globulin molecules. In contrast, simple geometrical considerations predict that forming larger protein particles should (i) increase the fraction of protein molecules shielded in the interior and (ii) substantially reduce the number of protein particles in suspension, thereby increasing the free space available to each.

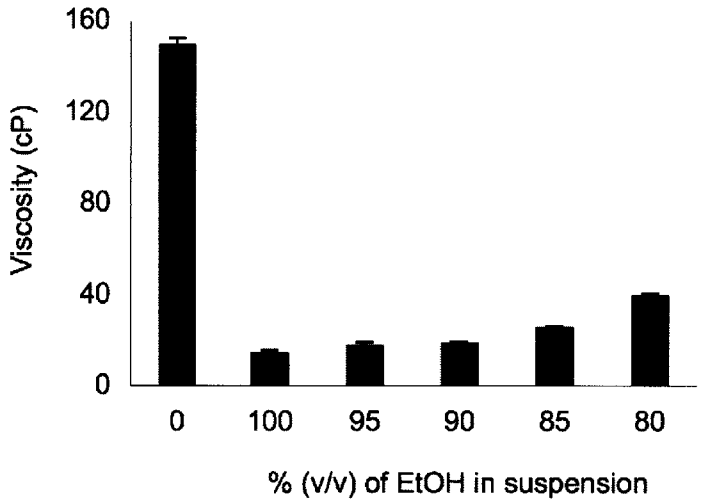

Figure 4-2. Viscosities at 25°C of a 260 mg/mL aqueous solution and aqueous-ethanol suspensions of γ-globulin. Solutions were prepared in 20 mM histidine-HCl buffer (final pH of 5.2) and suspensions using neat ethanol.

We observed a dense and opaque suspension when high concentrations of γ-globulin were precipitated in 80-100% (v/v) ethanol. These suspensions are thus comprised of particle much larger than nanoparticles. Therefore, we further examined the dependence of suspension viscosity on ethanol concentration. At 260 mg/mL, a γ-globulin suspension in neat (i.e., 100%) ethanol had the lowest viscosity: 15 ± 0.81 cP (Fig 4-2). Importantly, this is 9-fold lower than the viscosity of the corresponding aqueous solution of γ-globulin.

Examination of this γ-globulin suspension in neat ethanol by light microscopy revealed a wide distribution of particle sizes in the micron range, with a mean particle diameter of 8.9 μm (Table 4-7). In contrast to their much smaller counterparts discussed above, particles of this size should display only a small fraction of their component protein molecules on the surface, most being hidden in the interior of a particle. Additionally, such suspensions should have much larger inter-particle distances compared to nanosuspensions, let alone solutions, of γ-globulin.

Table 4-7. Viscosities at 25°C and protein particle sizes of a 260 mg/mL aqueous solution (final pH of 5.2) and neat ethanol suspension of cold-ethanol-precipitated γ-globulin.

Protein Preparation	Viscosity (cP)		Particle Diameter (um)	
	Solution	Suspension	Mean	Median
Commercial	150 ± 2.5	15 ± 0.81	8.9 ± 6.1	7.06
Ethanol-precipitated	140 ± 10	16 ± 1.3	9.6 ± 6.7	8.06

[a] Upon a 10-fold dilution, the distribution of particle sizes did not change (data not shown).

Enzymic proteins are remarkably stable when suspended in neat organic solvents[23], and we confirmed this principle for γ-globulin suspended in absolute ethanol. After removing the solvent under vacuum, and dissolving the dried protein powder in water, we measured that the original and post-suspension solution viscosities were similar, suggesting that under these conditions the protein suffers no irreversible solvent-induced unfolding and/or aggregation.

Figure 4-1 depicts the dependence of viscosity of γ-globulin suspensions in neat ethanol on protein concentration. The greatest drop in viscosity compared to the corresponding aqueous solution, 16-fold, is achieved at 300 mg/mL, the highest protein concentration examined. Therefore, though at all concentrations the viscosity of γ-globulin suspensions is lower than that of the solution, the higher the concentration the greater the advantage of suspension (Fig 4-1).

Enhancements in viscosity were also observed under certain temperature conditions. As the temperature was lowered from 25° to 10°C, viscosities of 260 mg/mL solution and ethanol suspension increased 3.0 and 1.7 fold, respectively (Fig 4-3). The same pattern holds for 300 mg/mL γ-globulin formulations, where solution and suspension viscosities at 25°C were 370 ± 17 cP and 23 ± 2.3 cP, respectively. At 17°C, the solution viscosity rose 1.8 fold, while that of the suspension increased only 1.3 fold (Fig 4-3). Therefore, maximal viscosity benefits from γ-globulin suspension in ethanol are observed at low temperature and high concentration.

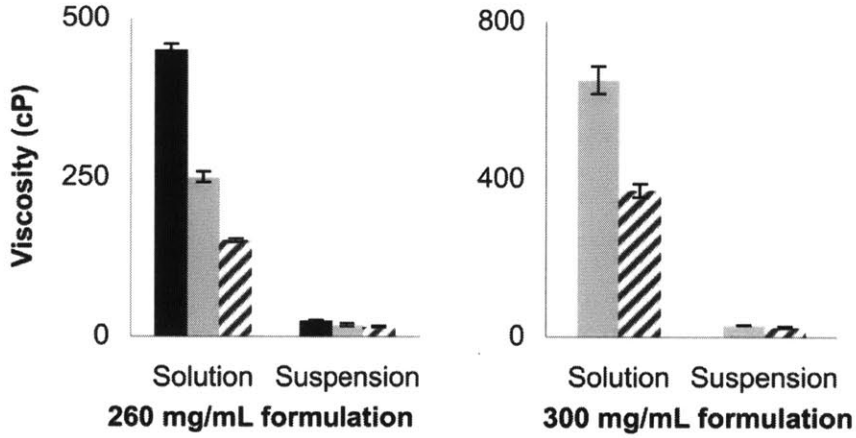

Figure 4-3. Temperature dependence of viscosities of γ-globulin suspensions of two different concentrations in neat ethanol measured at 10°C (black bars), 17°C (gray bars), and 25°C (hatched bars).

Thus far, all γ-globulin formulations were prepared from the solid protein as obtained from the manufacturer. Ideally, however, we would prepare γ-globulin powders in-house to control the process and ensure reproducibility. Therefore, we used cold-ethanol precipitation (a rapid isolation method widely used for antibody purification[21,22]), to prepare γ-globulin powder from the commercial one. As seen from the data in Table 4-7, cold-ethanol precipitation appears to cause no permanent damage; the resultant protein possessed nearly the same aqueous solution

and ethanol suspension viscosities as the commercial γ-globulin powder. Additionally, γ-globulin particle size in the resultant suspension (Table 4-7) was similar to that seen when a suspension was prepared from the commercial protein.

Hydrogen-bonding properties of organic solvents impact γ-globulin suspension viscosity

We next investigated the generality of our finding using the aforementioned cold-ethanol-precipitated γ-globulin. Suspensions of lysozyme in organic/oil mixtures were previously shown to produce low-viscosity formulations[14,24], although their viscosities were not directly compared to those of aqueous protein solutions. Here we selected over a dozen relatively simple neat organic solvents, and measured the viscosities of a 260 mg/mL suspension of γ-globulin in each of them (as well as the viscosities of the solvents themselves). As seen in Table 4-8, most of these protein suspensions were far less viscous than a γ-globulin solution in water. The tetrahydrofuran suspension had the lowest viscosity overall of only 3.6 cP: a 38-fold reduction compared to protein solution (Table 4-8). While tetrahydrofuran is not FDA-approved as a component of drug formulations, isopropanol is[25]; its 260 mg/mL γ-globulin suspension had 18-fold reduced viscosity compared to the corresponding protein solution.

Table 4-8. Viscosities at 25°C of 260 mg/mL suspensions of ethanol-precipitated γ-globulin in various neat organic solvents.[a]

Number of hydrogen atoms available for H-bonding	Solvent[b]	Viscosity (cP)	
		EtOH-precipitated powder	Solvent itself
≤ 1	**1**	3.6 ± 0.003	0.32 ± 0.01
	2	5.8 ± 0.50	0.46 ± 0.10
	3	6.3 ± 0.70	0.49 ± 0
	4	7.5 ± 0.24	0.33 ± 0.004
	5	7.7 ± 1.6	2.2 ± 0.11
	6	8.1 ± 1.3	1.9 ± 0.050
	7	12 ± 1.0	0.40 ± 0.010
	8	14 ± 1.6	1.72 ± 0.03
	9	15 ± 0.89	0.87 ± 0.010
	10	16 ± 1.3	1.1 ± 0.12
	11	25 ± 2.0	0.61 ± 0
	12	26 ± 1.0	7.8 ± 0.36
2	Water	140 ± 10	0.90 ± 0.010
	13	160 ± 6.5	48 ± 0.23
	14	200 ± 1.0	43 ± 0.10
	15	240 ± 23	55 ± 1.5

[a] The data for water has been included for comparison.

[b] The following solvents are FDA approved for use in IM/IV pharmaceutical formulations: **2**, **5-6**, **10**, **12-14**, and of course water. The remaining solvents are not approved for use (Ref 25).

Inspection of the data in Table 4-8 suggests that the viscosity roughly relates to the hydrogen-bonding ability of the solvent. Suspensions in those solvents (Fig 4-4) that are unable to donate a hydrogen atom for hydrogen-bonding (i.e., ethyl acetate, *N*-methylpyrrolidone, and toluene) or that possess only one such hydrogen (isopropanol, ethanol, and methanol) as a group have the lowest viscosities. Conversely, suspensions in solvents that contain two hydrogen atoms available for H-bond donation (PEG200, propylene glycol, 1,4-butanediol) all have viscosities over 6-fold higher. Thus, it appears that suspension in those solvent molecules that form the most extensive hydrogen-bonding with protein particles result in the greatest suspension viscosity; this rationale also applies to an aqueous solution of γ-globulin.

A recent publication[26] however, reported an opposite conclusion for three monoclonal antibodies suspended in miglyol, benzyl benzoate, and/or ethyl lactate (even though they observed no viscosity reduction benefits from suspending monoclonal antibodies in them). This difference is likely due to the fact that all three solvents tested were esters, thus providing little chemical diversity. The same conclusion applies to another 2012 publication[27].

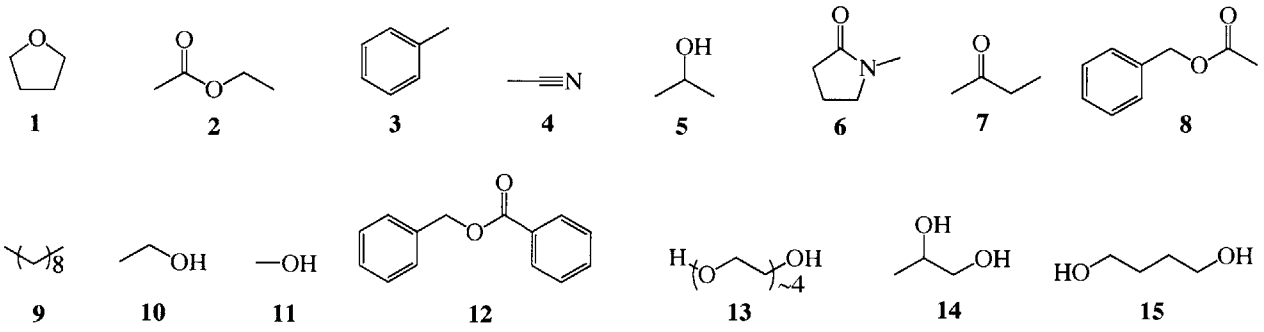

Figure 4-4. Chemical structures of organic solvents in which antibody powders were suspended. Tetrahydrofuran (**1**), ethyl acetate (**2**), toluene (**3**), acetonitrile (**4**), isopropanol (**5**), *N*-methylpyrrolidone (**6**), methyl ethyl ketone (**7**), benzyl acetate (**8**), decane (**9**), ethanol (**10**), methanol (**11**), benzyl benzoate (**12**), PEG 200 (**13**), propylene glycol (**14**), and 1,4-butanediol (**15**).

Viscosities of pharmaceutical antibody suspensions are also reduced in neat solvents

Murine, chimeric, humanized, and human IgG monoclonal antibodies comprise the majority of clinically validated therapeutics and experimental proteins[1,2]. Lastly, we explored the generality of the benefits of neat organic solvent suspensions (as presented in Table 4-8) by using a murine monoclonal antibody made at the pharmaceutical company Sanofi-Aventis (SMAb) and a humanized monoclonal antibody made at Novartis (NMAb). We first prepared a protein powder by concentrating and lyophilizing a SMAb solution. This dense solid was then milled to a fine powder in liquid nitrogen to minimize putative protein damage resulting from heat and/or moisture. Lyophilized powder dissolved rapidly in water and the resulting solution had increased viscosity, as expected, but showed no increase in protein particle diameter. After

concentration and liquid-nitrogen milling, SMAb powder again dissolved rapidly in water, though a portion of the solid was entirely insoluble.

An aqueous solution of the milled SMAb at 200 mg/mL had viscosity of 14 ± 0.75 cP (Table 4-9), very close to the 12 ± 0.14 cP for a solution of the non-milled powder (i.e., a SMAb solid obtained from direct lyophilization of the original 8.6 mg/mL solution). This suggests that the soluble milled protein was not damaged or aggregated as a result of liquid nitrogen milling. Aggregation or unfolding could be particularly problematic with therapeutic antibodies as these changes decrease affinity and increase the incidence of immunogenicity *in vivo*[28]. We then suspended this milled SMAb powder in toluene – a solvent that gave one of the lowest suspension viscosities in γ-globulin studies (Table 4-8) – at the same 200 mg/mL concentration. The toluene suspension viscosity was 4.9 ± 0.68 cP (Table 4-9), 2.5-fold reduced from the solution.

Table 4-9. Viscosities at 25°C of aqueous solutions of SMAb (120 mg/mL, final pH of 5.2) and NMAb (150 mg/mL, final pH of 6.1), and SMAb and NMAb suspensions in neat toluene or ethanol, respectively.

Protein preparation	Viscosity (cP)	
	SMAb[a]	NMAb[b]
Solution	12 ± 0.14	74 ± 2.4
N_2-Milled MAb solution[c]	14 ± 0.75	86 ± 4.0
N_2-Milled MAb suspension[c]	4.9 ± 0.68[c]	11 ± 1.5

[a] SMAb was formulated at 120 mg/mL in sodium citrate buffer or toluene. It was not possible to examine more concentrated preparations because solid MAb at 200 mg/mL comprised almost the entire volume of the suspension in organic solvents. A minor portion of the milled SMAb was insoluble in water, presumably due to irreversible aggregation. Protein concentration was determined by measuring absorbance at 280 nm.

[b] NMAb was formulated at 150 mg/mL in histidine-HCl bufer or ethanol.

[c] "N2-milled" refers to solid MAb obtained by milling in liquid nitrogen.

A second, humanized MAb was obtained from the pharmaceutical company Novartis and at a concentration of 150 mg/mL had a viscosity of 74 ± 2.4 cP (Table 4-10). When lyophilized and milled, the viscosity of an ethanolic suspension of this NMAb was 8.5-fold less than that of the corresponding solution. Both MAbs demonstrate the same trends: 1) fine and homogenous powder forms low viscosity suspensions and 2) suspension in either hydrophilic or hydrophobic solvents decreases formulation viscosity.

Conclusion

In this work, we successfully endeavored to lower the viscosities of concentrated antibody formulations by switching from solutions to suspensions of amorphous powders. Methods to prepare low-viscosity suspensions of the model protein γ-globulin and full-length murine and humanized MAbs in organic solvents were elaborated and validated. Protein-protein and protein-solvent hydrophobic, electrostatic, and hydrogen-bonding interactions were identified as critical in the observed viscosity reductions. By suspending protein powders in organic solvents possessing one or no hydrogen atoms available for H-bonding, we prepared highly concentrated but still non-viscous antibody formulations.

Acknowledgements

I would like to thank Dr. Charu Srinivasan for collaborating on this work and for performing the foundational studies on this project. I am grateful to Dr. Peter Bak for taking the time to assist with microscopy studies. I also thank Debbie Pheasant of the MIT Biophysical Instrumentation Facility for the Study of Complex Macromolecular Systems (funded by NSF-0070319 and NIH GM68762 instrumentation grants) for her assistance and thoughtful conversations.

C. Materials and Methods

Chemicals

Monoclonal antibody designated herein as SMAb was kindly provided by Sanofi-Aventis Company (Frankfurt, Germany). The 147-kDa murine SMAb with an isoelectric point of 6.6 was supplied at 8.6 mg/mL in 10 mM citrate buffer (pH 5.5). Monoclonal antibody designated herein as NMAb was kindly provided by Novartis Pharma AG (Basel, Switzerland). Properties of the humanized NMAb can be found in Reference 7, where it is designated as "MAb 1". Bovine γ-globulin (product #G5009), other reagents, and most solvents were purchased from Sigma-Aldrich Chemical Co. (St. Louis, MO); absolute ethanol was from VWR International (Radnor, PA).

Viscometry

Viscosities were measured using a Brookfield DV-II Pro viscometer equipped with a cone-and-plate geometry, a CPE 40 or CPE 52 spindle, and a temperature-controlling water bath. The viscometer was pre-calibrated using a CAP0L standard (supplied by Brookfield) and water. Measurements were performed with 500-μL samples in the "external" mode, where increasing shear rates equivalent to10%-100% of instrument torque (from 3.0 to 53 s^{-1} and 23 to 200 s^{-1}) were used, depending on viscosity. The viscosity values reported herein are an average of at least duplicate measurements taken at 25°C unless stated otherwise. Plots of viscosity *vs.* shear rate were typically non-linear, characteristic of non-Newtonian pseudoplastic solutions and suspensions[29] (Fig 4-5A); however, such solvents as ethanol and ethyl acetate, when measured alone as controls, exhibited ideal Newtonian behavior (Fig 4-5B). All protein formulations exhibited a non-Newtonian dependence, as expected for concentrated solutions and colloidal suspensions[30,31]. The resultant plots were extrapolated to zero-shear values from the highest

three shear rates[13,29]. Apparent viscosities calculated from these linear extrapolations were accepted when the R^2 exceeded 0.95[29].

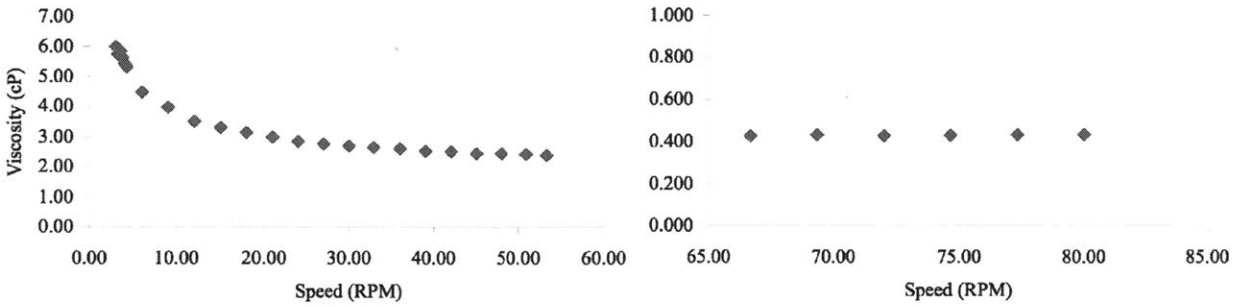

Figure 4-5. Sample plots of viscosity vs. speed for a non-Newtonian SMAb solution (**A**) and Newtonian organic solvent ethyl acetate (**B**).

Dynamic light scattering

Particle diameters of γ-globulin nanosuspensions were measured using a DynaPro NanoStar Light Scattering instrument from Wyatt Technology (Santa Barbara, CA) in the dynamic light scattering mode. Measurements were performed in duplicate according to manufacturer's instructions in a quartz cuvette at a laser wavelength of 658 nm. Particle diameters were determined using % mass analysis. Typically, the population of interest comprised >98% by mass for dilute formulations and >93% by mass for concentrated formulations.

Light microscopy

Particle diameters of micron-sized γ-globulin suspensions were measured using a Zeiss Axioplan II upright microscope with a halogen transmitted light source. Images were collected with a Qimging color camera at 10- and 25-fold magnifications. A protein suspension in 2 μL of ethanol was smeared across a glass microscope slide, quickly covered with a No. 1 glass cover

slip and immediately sealed with nail polish to prevent evaporation of ethanol. ImageJ software was used to determine the average diameter of ~200 protein particles per sample.

Preparation of γ-globulin solutions, suspensions, and nanosuspensions

γ-Globulin aqueous solutions were prepared at the desired concentration by adding water or aqueous buffer to protein powder, followed by centrifugation at 1,300 x *g* for 60 min using an Eppendorf 5810R centrifuge equipped with an A-4-81 rotor. Volume was adjusted as necessary: for example, only 3.5 mL of water was added to 1.3 g of γ-globulin to prepare 5 mL of protein solution at 260 mg/mL. A stir bar was added, and the resulting mixture was gently shaken overnight at room temperature to achieve complete dissolution of the protein. The pH of this solution was 6.0 unless otherwise indicated. Subsequently, the γ-globulin solution was centrifuged at 500 x *g* for 10 min to remove air bubbles prior to viscosity measurements.

To make protein nanosuspensions using such precipitating agents as 4,000-Da poly(ethylene glycol) (PEG4000), a solution of γ-globulin was prepared with a final volume below 5 mL. PEG4000 was then added to the desired concentration (w/v), and the mixture at room temperature was gently stirred for 1 h to dissolve the PEG4000, and centrifuged at 500 x *g* for 10 min to remove air bubbles. Volume was then adjusted as necessary.

An analogous protocol was used to make aqueous suspensions with ethanol: To prepare aqueous ethanolic suspensions of γ-globulin, neat ethanol was added to a concentrated γ-globulin solution prepared as described above to give a final ethanol concentration in the range of 80-95% (v/v) and a final γ-globulin concentration of 260 mg/mL.

To prepare γ-globulin suspensions in neat organic solvents, the latter was added to protein powder to the desired concentration (e.g., 5 mL to 1.3 g). The mixture was centrifuged at 1,300 x *g* for 10 min. A stir bar was introduced, and the suspension was tapped to release the

thick protein pellet and stir bar. The resultant suspension was gently shaken for 3 h at room temperature and centrifuged at 500 x *g* for 10 min. The volume was adjusted as necessary, and the suspension was stirred for 5 min at room temperature to re-suspend protein particles before viscosity measurements. The same viscosities were observed whether the suspension was formed by adding solvent to γ-globulin or *vice versa*.

Ethanol precipitation of γ-globulin

Ethanol precipitation of γ-globulin was performed in a cold room from a 260 mg/mL protein solution prepared as described above with both liquids chilled to 4°C. The final ratio of absolute ethanol to protein solution was 4:1 (v/v). The first portion of cold ethanol was added drop-wise to a protein solution with vigorous stirring. The remaining three portions were added in a slow stream. The resultant mixture was stirred for 10 min and filtered through a Corning Disposable Sterile Filter System with a 0.22-μm-pore polyethersulfone membrane. After 10 min, the collected solid (which should be slightly sticky but not wet) was disturbed and left on the filter to dry. After another 5 min, the solid was transferred from the filter to a weigh paper and dried for 1 h. During this drying step, the solid was repeatedly flattened and then scraped up in order to help release trapped ethanol to result in a white, very fine, free-flowing powder.

Preparation of solid MAb

Solid SMAb was prepared from the buffered aqueous solution in which it was received from Sanofi-Aventis by concentration, lyophilization, and liquid-nitrogen milling. First, it was spin-concentrated to approximately 200 mg/mL in a 50-kDa MWCO Amicon Ultra-15 device (EMD Millipore) with a regenerated cellulose membrane. The concentrated solution was flash frozen and lyophilized for up to 48 h until dryness. A mortar and pestle were placed in a crystallization dish and pre-cooled in liquid nitrogen. Solid SMAb was placed in the mortar and

frozen for 10 min. Next, the protein was milled for 10 min; liquid nitrogen was added to the mortar and dish as needed to prevent crystallization of water within the mortar and on the end of the pestle. It is important to note that concentration *and* milling were necessary to form a protein powder fine enough to suspend at high concentration. After milling, the suspended protein was poured into a glass scintillation vial and covered with a Kimwipe™ to allow the liquid nitrogen to evaporate. The solid SMAb was then stored at 4°C for short-term use. Solid NMAb was prepared and stored analogously, with lyophilization directly from the provided solution.

Preparation of solutions and suspensions of MAb

Aqueous solutions were prepared by incrementally adding solid MAb powder to an appropriate volume of water or aqueous buffer in a 1.5-mL Eppendorf tube (solvent was chosen to give the same citrate concentration in all samples). The mixture was centrifuged in a VWR Galaxy 7 Microcentrifuge at 1,500 rpm for 1 min and then gently shaken at room temperature until near-complete dissolution occurred (typically 30-60 min). Additional powder was added and the process repeated until the final concentration of protein – as determined by absorbance at 280 nm – was achieved.

To prepare MAb suspensions in neat organic solvent, protein powder was added to a 5-fold (w/v) excess of solvent in a 15-mL Falcon tube. The mixture was centrifuged at 1,000 x *g* for 10 min using an Eppendorf 5810R centrifuge equipped with an A-4-81 rotor and then gently shaken for 1 h at room temperature. The protein was pelleted at 2,500 x *g* for up to 10 min and the solvent aspirated. Fresh solvent was added to the desired concentration (as determined by the total volume of the suspension: the sum of the volumes of liquid and the pelleted solid). The powder was resuspended by gentle shaking for 5 min immediately prior to viscosity measurements.

D. References

1. Beck A, Wurch T, Bailly C, Corvaia N, Strategies and challenges for the next generation of therapeutic antibodies. *Nature Revs Immunol*, **2010**, 10, 345-352.
2. Weiner LM, Surana R, Wang S, Monoclonal antibodies: versatile platforms for cancer immunotherapy. *Nature Revs Immunol*, **2010**, 10, 317-327.
3. Ahamed T, Esteban BNA, Ottens M, van Dedem GWK, van der Wielen LAM, Bisschops MAT, Lee A, Pham C, Thommes J, Phase behavior of an intact monoclonal antibody. *Biophys J*, **2007**, 93, 610-619.
4. Keizer RJ, Huitema AD, Schellens JH, Beijnen JH, Clinical pharmacokinetics of therapeutic monoclonal antibodies. *Clin Pharmacokinet*, **2010**, 49, (8), 493-507.
5. Mascelli MA, Zhou H, Sweet R, Getsy J, Davis HM, Graham M, Abernethy D. *J Clin Pharmacol* **2007**, 47, (5), 553-565.
6. Hansel TT, Kropshofer H, Singer T, Mitchell JA, George AJ, The safety and side effects of monoclonal antibodies. *Nat Rev Drug Discov*, **2010**, 9, (4), 325-338.
7. Hendeles L, Sorkness CA, Anti-immunoglobulin E therapy with omalizumab for asthma. *Ann Pharmacother*, **2007**, 41, (9), 1397-1410.
8. Frokjaer S, Otzen DE, Protein drug stability: a formulation challenge. *Nature Revs Drug Discov*, **2005**, 4 ,298–306.
9. Kremer J, Ritchlin C, Mendelsohn A, Baker D, Kim L, Xu Z, Han J, Taylor P, Gaolimumab, a new human anti-tumor necrosis factor alpha antibody, administered intravenously in patients with active rheumatoid arthritis: Forty-eight-week efficacy and safety results of a phase III randomized, double-blind, placebo-controlled study. *Arthritis Rheum*, **2010**, 62, (4), 917-928.
10. Yang MX, Shenoy B, Disttler M, Patel R, McGrath M, Pechenov S, Margolin AL, Crystalline monoclonal antibodies for subcutaneous delivery. *Proc Natl Acad Sci USA*, **2003**, 100, 6934-6939.
11. Shire SJ, Shahrokh Z, Liu J, Challenges in the development of high protein concentration formulations. *J Pharm Sci*, **2004**, 93, 1390-1402.
12. Du W, Klibanov AM, Hydrophobic salts markedly diminish viscosity of concentrated protein solutions. *Biotechnol Bioeng*, **2011**, 108, 632-636.
13. Guo Z, Chen A, Nassar RA, Helk B, Mueller C, Tang Y, Gupta K, Klibanov AM, Structure-activity relationship for hydrophobic salts as viscosity-lowering excipients for concentrated solutions of monoclonal antibodies. *Pharm Res*, **2012,** 29, 3102-3109.
14. Miller MA, Engstrom JD, Ludher BS, Johnston KP, Low viscosity highly concentrated injectable nonaqueous suspension of lysozyme microparticles. *Langmuir*, **2010**, 26, 1067-1074.
15. Johnston KP, Maynard JA, Truskett TM, Borwankar AU, Miller MA, Wilson BK, Dinin AK, Kjan TA, Kaczorowski KJ, Concentrated dispersion of equilibrium protein nanoclusters that reversibly dissociate into active monomers. *ACS Nano*, **2012**, 6, 1357-1369.
16. Basu SK, Govardhan CP, Jung CW, Margolin AL, Protein crystals for the delivery of biopharmaceuticals. *Expert Op Biol Ther*, **2004**, 4, 301-317.
17. Kanai S, Liu J, Patapoff HW, Shire SJ, Reversible self-association of a concentrated monoclonal antibody solution mediated by Fab-Fab interaction that impacts solution viscosity. *J Pharm Sci*, **2008**, 97, 4219-4227.

18. Yadav S, Shire SJ, Kalonia DS, Factors affecting the viscosity in high concentration solutions of different monoclonal antibodies. *J Pharm Sci*, **2010**, 99, 4812–4829.
19. Patel HM, Kraszewski JL, Mukhopadhyay B, The phosphoenolpyruvate carboxylase from *Methanothermobacter thermautotrophicus* has a novel structure. *J Bacteriol*, **2004**, 186, 5129-5137.
20. Matheus S, Friess W, Schwartz D, Mahler H-C, Liquid high concentration IgG1 antibody formulations by precipitation. *J Pharm Sci*, **2009**, 98, 3043-3057.
21. Englard S, Seifter S, Precipitation techniques. *Meth Enzymol*, **1990**, 182, 285-300.
22. Van Oss CJ, On the mechanism of the cold ethanol precipitation method of plasma protein fractionation. *J Protein Chem*, **1989**, 8, 6661-6668.
23. Klibanov AM, Improving enzymes by using them in organic solvents. *Nature*, **2001**, 409, 241-246.
24. Foster TP, Moseley WM, Caputo JF, Alaniz GR, Leatherman MW, Yu X, Claflin WH, Reeves DR, Cleary DL, Zantello MR, Krabill LF, Wiest JR, Sustained elevated serum somatotropin concentrations in Holstein steers following subcutaneous delivery of a growth hormone releasing factor analog dispersed in water, oil or microspheres. J *Control Rel*, **1997**, 47, 91-99.
25. FDA. Inactive ingredient search for approved drug products. November 23, 2012. Available from: http://www.accessdata.fda.gov/scripts/cder/iig/index.cfm
26. Bowen M, Armstrong N, Ma Y-F, Investigating high-concentration monoclonal antibody powder suspension in nonaqueous suspension vehicles for subcutaneous injection. *J Pharm Sci*, **2012**, 101, 4433-4443.
27. Dai W, Hill B, Liu K, Mieczkowski C, Non-aqueous high concentration reduced viscosity suspension formulations of antibodies. US Patent Application **2012**, 0 076 800.
28. Saluga A and Kalonia DS, Nature and consequences of protein-protein interactions in high protein concentration solutions. *Int J Pharm*, **2008**, 358, (1-2), 1-15.
29. He F, Becker GW, Litowski JR, Narhi LO, Brems DN, Razinkov VI, High throughput dynamic light scattering methods for measuring viscosity of concentrated protein solutions. *Anal Biochem*, **2010**, 399, 141-143.
30. Krieger IM, Dougherty TJ, A mechanism for non-Newtonian flow in suspensions of rigid spheres. *Trans Soc Rheol, **1959***, 3, 137-152.
31. Patel AR, Kerwin BA, Kanapuram SR, Viscoelastic characterization of high concentration antibody formulations using quartz crystal microbalance with dissipation monitoring. *J Pharm Sci*, **2009**, 98, 3108-3116.

Appendix

α-D-*glycero*-D-*galacto*-*(nonulopyranoside)onic acid*
*(sialic acid derivative **10**)*

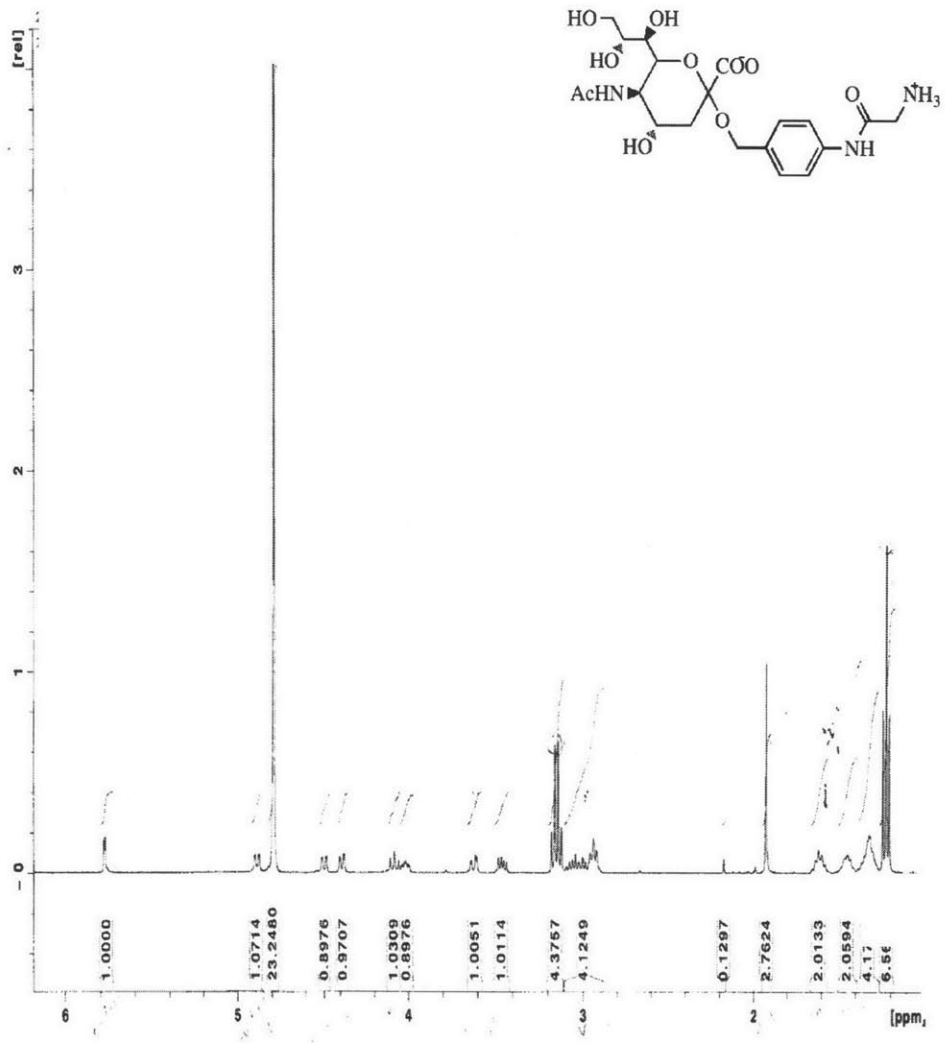

(4S, 5R 6R)-5-Acetylamino-6-{1R-[(6-aminohexyl)-carbamoyloxy]-2R,3-dihydroxypropyl}-4-guanidino-5,6-dihydro-4H-pyran-2-carboxylic acid
*(zanamivir derivative **11**)*

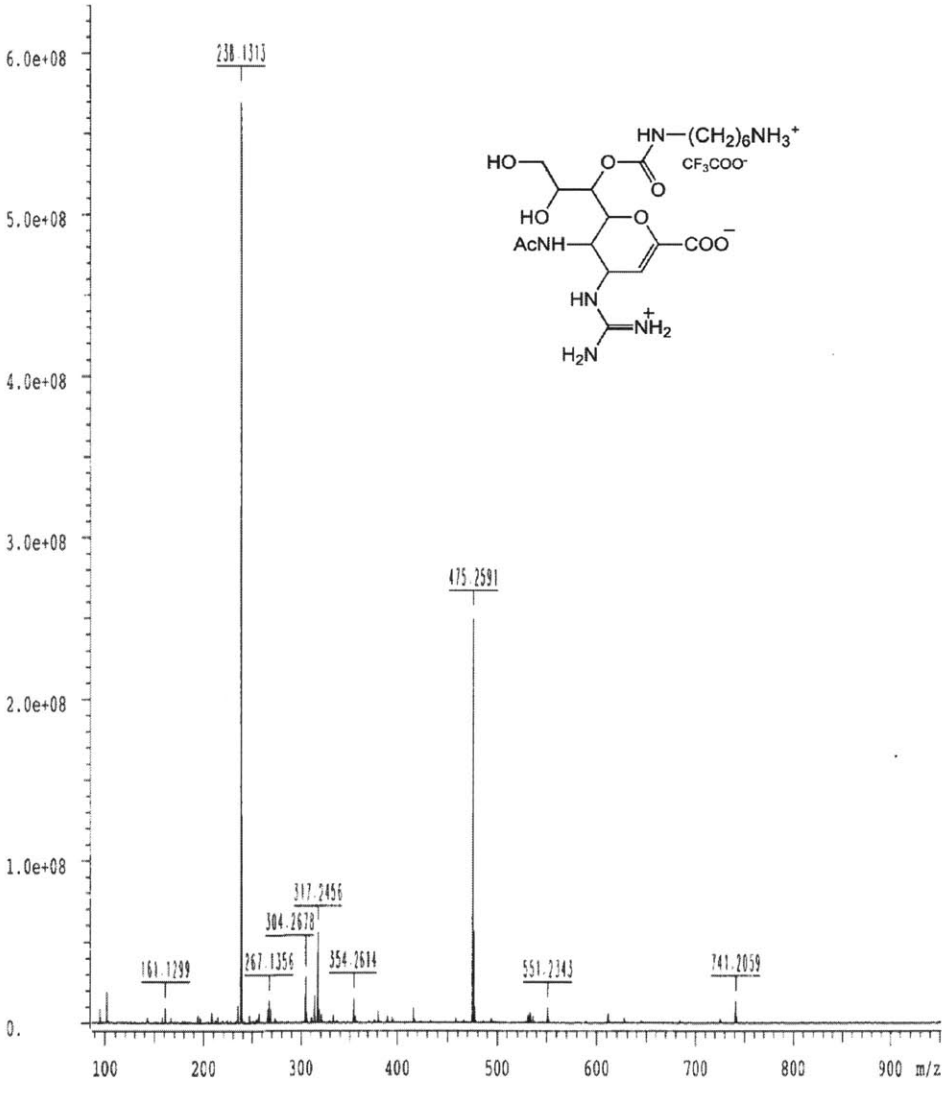

*3-Acetamido-2-(1-(((4-(aminomethyl)phenyl)carbamoyl)oxy)-2,3-dihydroxypropyl)-4-guanidino-3,4-dihydro-2H-pyran-6-carboxylic acid (**14**)*

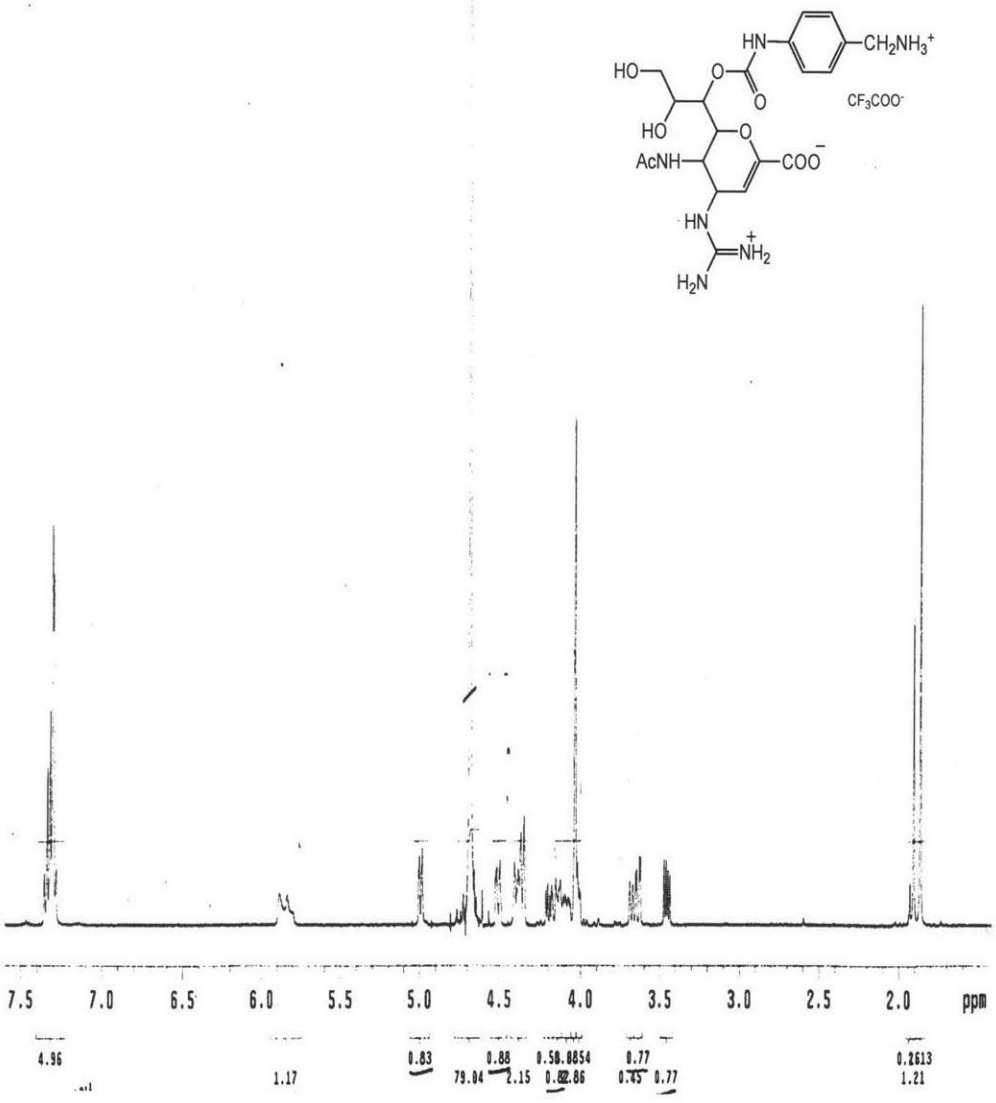

*3-Acetamido-2-(1-(((2-(2-aminoethoxy)ethyl)carbamoyl)oxy)-2,3-dihydroxypropyl)-4-guanidino-3,4-dihydro-2H-pyran-6-carboxylic acid (**13**)*

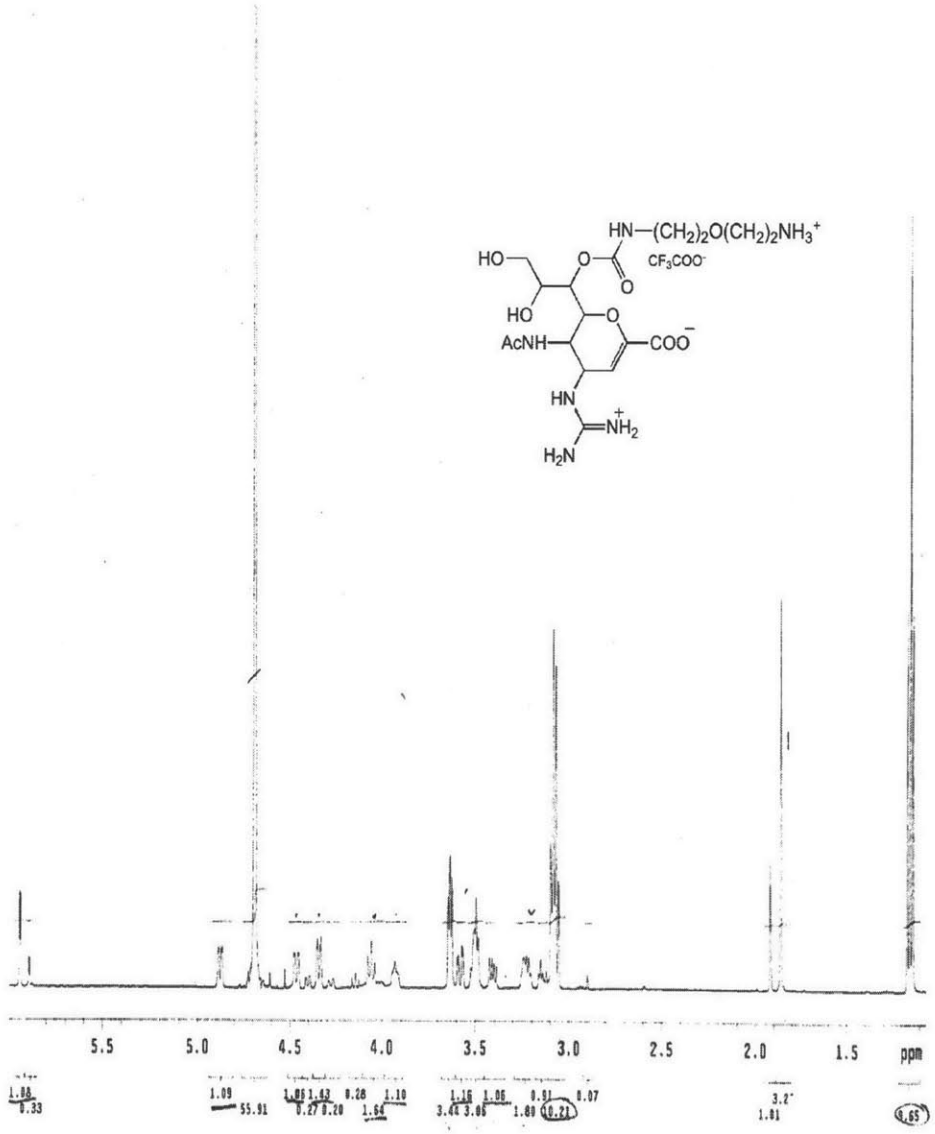

Poly-L-*glutamine derivatized with 5% zanamivir* (***12h***)

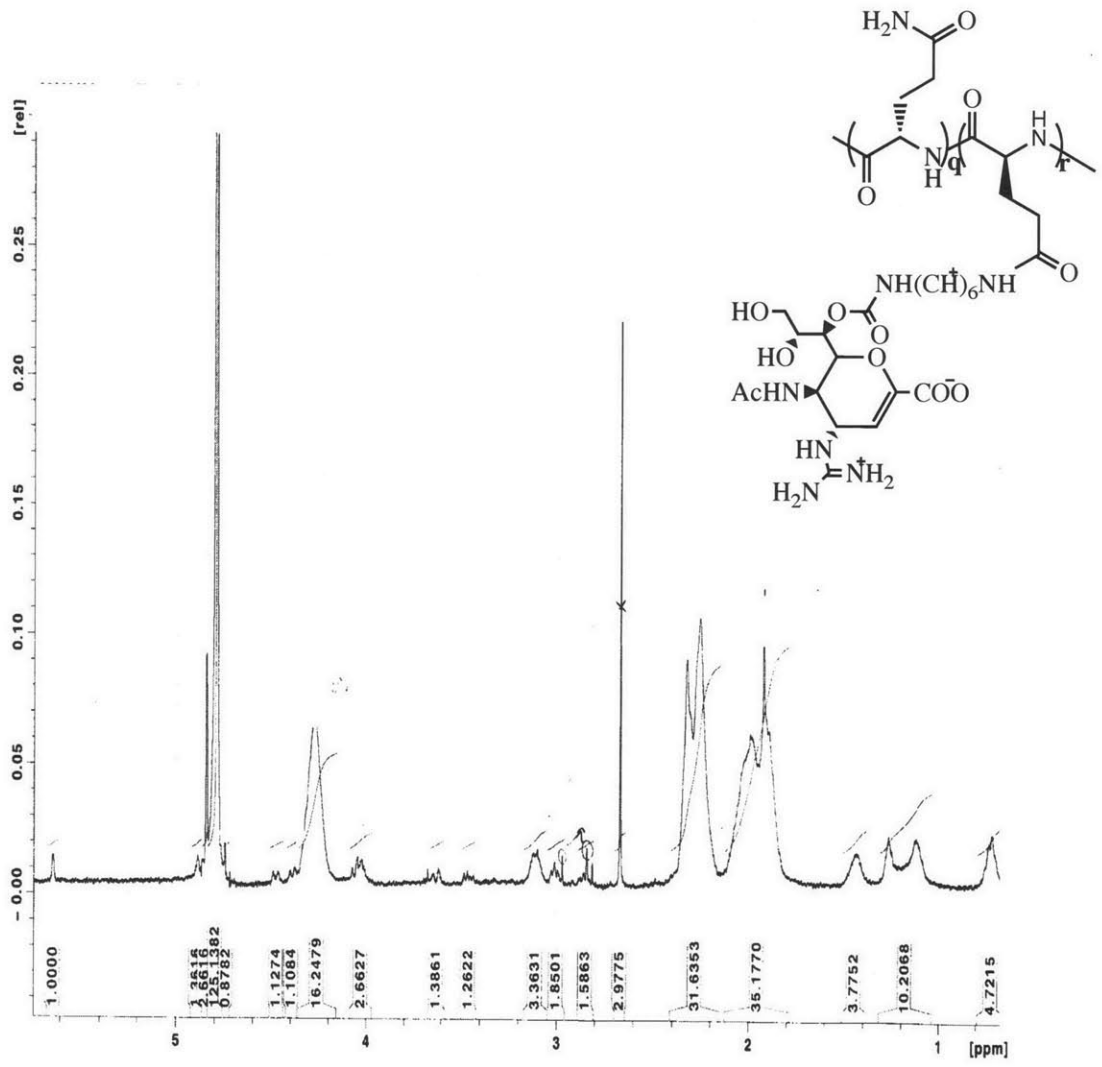

Zwitterionic polymer scaffold ***16a****: 2-methoxy-N,N,N-trimethylethanaminium and free carboxylate side chains*